

Article

Experimental Verification of 1D-Simulation Method of Water Hammer Induced in Two Series-Connected Pipes of Different Diameters: Determination of the Pressure Wave Speed

Mariusz Lewandowski *  and Adam Adamkowski 

The Szewalski Institute of Fluid-Flow Machinery, Polish Academy of Sciences, 14th Fiszerza St., 80-231 Gdańsk, Poland; adam.adamkowski@imp.gda.pl

* Correspondence: mariusz.lewandowski@imp.gda.pl

Abstract: This paper presents the results of laboratory tests of water hammer phenomenon induced in two series-connected copper pipes with different diameters (a diameter ratio of 1:1.25) by a quick-closing valve installed at the end of the simple upstream tank–pipeline–valve system. Test results were compared with calculations made with the use of various friction loss models incorporated in a one-dimensional model based on a method of characteristics. The calculation takes into consideration quasi-steady and unsteady friction models as well as a special discretization procedure of the solution domain that ensures the elimination of numerical diffusion in the numerical scheme. The main attention was paid to determining the value of the pressure wave speed in the pipes, which has a significant influence on the compliance between the calculations and the experimental results of the pressure amplitudes and wave frequencies. Two methods of determining the wave speed were proposed and evaluated based on the measurements. The results presented in this article indicate that the use of the proposed procedure instead of the classic formulas for determining the pressure wave speed gives the desired correspondence between the frequencies of the measured and calculated waves. Calculation examples made with the use of different friction models showed that application of the developed procedure for discretization of the solution domain and the method used for determining the wave speed opened the possibility of reliable verification of these models, free of numerical errors and frequency discrepancies between the computational and measured wave.

Keywords: water hammer; pressure wave speed; unsteady friction losses modelling; pipeline systems of series-connected pipes; equivalent pipeline systems



Citation: Lewandowski, M.; Adamkowski, A. Experimental Verification of 1D-Simulation Method of Water Hammer Induced in Two Series-Connected Pipes of Different Diameters: Determination of the Pressure Wave Speed. *Appl. Sci.* **2024**, *14*, 7173. <https://doi.org/10.3390/app14167173>

Academic Editor: Rui M.L. Ferreira

Received: 21 June 2024

Revised: 28 July 2024

Accepted: 12 August 2024

Published: 15 August 2024



Copyright: © 2024 by the authors. Licensee MDPI, Basel, Switzerland. This article is an open access article distributed under the terms and conditions of the Creative Commons Attribution (CC BY) license (<https://creativecommons.org/licenses/by/4.0/>).

1. Introduction

The vast majority of water hammer laboratory tests concern pipelines with constant cross-sections. There are many examples in the literature of different kinds of simulation models based on the measurement results of pressure wave propagation in such pipelines. These models concern friction loss [1–4], column separation and transient cavitation [5–9], FSI and visco-elasticity of pipeline materials [10–14], as well as transient flow of liquids in pipelines with air content [15–18]. The use of pipelines with constant diameters in these examples allowed the avoidance of, among others, considering different pressure wave parameters characteristic of individual pipes with different diameters connected in series. Flow conditions in such pipes that make up a complex system are characterized with different liquid flow velocities, as well as different pressure wave propagation speeds. These parameters significantly affect the parameters of the numerical model and thus the obtained calculation results. This is a particularly important issue when using the method of characteristics (MOC), in which the selection of the numerical grid requires a special approach to eliminate the influence of numerical damping on the calculation results that is crucial when the purpose is to verify the friction models used in the calculations. In such a situation, the aim should be to obtain calculation results free of e.g., numerical damping,

which requires an appropriate approach to discretization of the solution area together with precise knowledge of the wave propagation speed in all elements of a complex flow system.

Since this type of issue is often analyzed in the setting of engineering practice, in some research it is recommended to replace pipelines composed of different pipes connected in series with one pipe with a constant, equivalent diameter with respect to wave speed, inertia forces and pressure losses [19–23]. This approach is particularly useful in the simulation of transient phenomena in complex transmission networks, where connections of pipes of different diameters are usually very common. Therefore, both from the theoretical and practical point of view, there is a need to know how reliable such an approach is.

The available literature shows that in recent decades, numerous researchers have paid attention to the study of transients in pipelines composed of pipes of variable diameters and different materials [24–33]. In the publications of [25–29], the results of studies of unsteady liquid flow in the viscoelastic pipeline system with variable diameters and materials are considered. In [32,33] a method based on the analysis in the frequency domain of determining the equivalent speed in the pipeline system consisting of different pipes connected in series has been introduced. This method can also be found in the [34] monograph.

Authors of [24] investigated numerically the effect of a narrowed section of an elastic pipeline on a water hammer using the MOC method. Transient friction losses were taken into account using the Zielke friction model applicable for laminar flow, which is very rare in engineering practice.

In [30], the MacCormack scheme for a system of elastic pipes connected in series is used to solve the equations describing the water hammer. The Brunone model was used in the friction loss calculations. The obtained results were compared with the results obtained using the MOC, while the comparison with the results from the experiment was made only for a single pipeline with constant parameters (concerning geometry and wave) along its length.

In [31], a mathematical model for calculating the course of a water hammer in a system of elastic (steel) pipes connected in series is presented. In the numerical simulations, the MacCormack scheme was also used, assuming a constant pressure wave speed equivalent to a given pipe configuration, and the calculation of friction losses was based on the Brunone model. The calculations were experimentally verified by adjusting the parameters of the adopted friction model.

In the context of pipelines of variable diameter, attention should also be paid to a number of works whose main purpose is to detect extended blockages in pipelines using the nature of transient pressure wave waveforms (i.e., transient test-based techniques). Most often, the physical model in this issue is a section with a smaller diameter inserted into the pipeline, and in order to detect blockages, an analysis of pressure changes is carried out in the frequency domain [35–41] or in the time domain [25,42–44]. Techniques for detecting blockages in pipelines are also proposed based on the coupling of these two approaches, i.e., on transient tests analyzed in the frequency domain and time domain [45]. Both experimental and numerical tests are used to validate the detection techniques. Numerical tests are prepared using MOC or other methods of solving equations describing the water hammer in pipelines with constrictions simulating extended blockages.

On the basis of the available publications, it should be noted that the results of the numerical simulation of the water hammer with the use of various models of friction losses for elastic pipelines connected in series and the comparison of these results with the results of experimental tests are not very frequent. Examples of articles that present such results analyze the issues of numerical errors generated by the calculation scheme in a superficial and insufficient way. Also, the issue of determining the pressure wave speed in individual pipes of a complex flow system is not the subject of thorough analysis. Typically, the proposed solutions are based on classical methods of estimating the pressure wave speed and ignore the impact of these methods on the calculation results.

The main purpose of work presented in this paper was to conduct laboratory tests of a water hammer in a relatively simple pipeline system composed of two copper pipes

connected in series with different diameters and relative wall thicknesses. The results of these tests were used to verify the developed numerical method for simulating a water hammer, which takes into account different models of friction losses. In order to ensure the appropriate conditions for such verification, the method, based on MOC, includes a special procedure allowing for the avoidance of numerical damping.

The basis of this method is the precise determination of the pressure wave speed for each of the pipes in the complex flow system. This is necessary to select the appropriate size of the numerical grid, which for the determined wave speeds will ensure the calculation results without numerical attenuation.

Considering the pipes in the flow system as thin walled, the calculation of the pressure wave speed in its individual pipes can be based on the following formula [19]:

$$a_{i_calc} = \sqrt{\frac{K}{\rho \left(1 + \frac{K D_i}{E_i e_i} c_{1_i}\right)}} \quad (1)$$

where a_{i_calc} is the computational pressure wave speed in the i -th pipe [m/s], K is the liquid elasticity modulus [Pa], E_i is the Young's modulus for the material of the i -th pipe [Pa], ρ is the liquid density [kg/m³], D_i is the internal diameter of the i -th pipe [m] and e_i is the wall thickness of the i -th pipe [m]. The coefficient c_{1_i} [-] depends on the method of fixing the i -th pipe:

- $c_{1_i} = 1 - 0.5\nu_i$ for a pipe anchored at its one end only;
- $c_{1_i} = 1 - \nu_i^2$ for a pipe anchored throughout from axial movement;
- $c_{1_i} = 1$ for a pipe anchored with expansion joints throughout.

where ν_i [-] is the Poisson's ratio of the i -th pipe material.

Calculation of the pressure wave speed using Equation (1) may be associated with even a few (or more) percent inaccuracy, influenced by the underlying assumptions [46]. According to them:

- The influence of FSI on the pressure wave propagation speed change is not taken into account. Only the quasi-static response of the pipeline structure to the pressure wave is taken into account;
- The bulk modulus of the liquid is constant, regardless of pressure changes;
- Changes in liquid density due to pressure are not taken into account—e.g., it is assumed that the liquid is not a water–gas mixture;
- A two-dimensional state of stress in the pipeline shell is assumed (thin wall pipe);
- The manner and influence of the pipeline support and fastening on the pressure wave speed is taken into account by using an approximate value of the c_1 coefficient.

With the appropriate configuration of the flow system and rigid mounting of the pipelines, the influence of FSI on the pressure wave speed can be eliminated or at least significantly reduced. The variability of the compressibility modulus and density from pressure for a fluid consisting of a mixture of water and a small amount of air may also be an insignificant concern for the pressure wave speed. The assumption of treating the pipeline as thin walled depends on the D_{outer}/e ratio. It is usually assumed that pipelines with a D_{outer}/e ratio not lower than 20 can be treated as thin walled, which means that assuming a two-dimensional state of stress in such cases affects the determination of the value of the pressure wave speed insignificantly. The last mentioned factor related to the fastening of the pipeline and the corresponding correct value of the c_1 coefficient most significantly affects the uncertainty of a estimated using Equation (1).

In connection with the assumptions underlying Equation (1), in order to make the most reliable verification of the developed numerical calculation method in this work, the determination of the pressure wave speed for a system consisting of pipe series of different diameters was based on the measured and recorded pressure changes induced by a sudden flow cut-off. Two methods for determining pressure wave speed a_i , characteristic for the

particular pipes forming the system, were proposed and used in the numerical analysis of the water hammer phenomenon.

The following parts of the paper describe the numerical method used to simulate the water hammer phenomenon in complex systems, which takes into account the quasi-steady and unsteady models of friction losses. This method uses an original procedure of discretization of the solution domain, which allows for avoiding the artificial damping generated, usually by the numerical scheme. This is particularly important for the accurate verification of the friction loss models used in the calculations.

The mathematical model forming the basis of the numerical method was verified using qualitative comparative analysis between the measurement and calculation results. The conclusions provided a basis for evaluating the friction loss models used in the calculations according to the agreement of the calculation and experimental results. The simplified approach to calculating the course of pressure changes during a water hammer, involving the use of equivalent quantities, was also evaluated.

The problem related to the occurrence of the water hammer phenomenon concerns most technological systems encountered in practice. Wherever these systems are built from pressure pipelines, this phenomenon should be absolutely taken into account at the conceptual and design stage. Additionally, special attention should be paid to it during the current operation of such systems by designing appropriate operating procedures to prevent the adverse effects of the occurrence of a water hammer and to ensure the work safety of these systems. Pipeline systems cooperating with pumps, penstocks of hydropower plants, and long transport pipelines in which numerous regulating and shut-off fittings are installed, which may cause this phenomenon, are particularly vulnerable to the formation of a water hammer. Such systems are usually built from numerous connections of variable diameter pipelines and branches, which significantly complicate the analysis of flow phenomena, including water hammers. Therefore, it is so important to recognize the influence of the geometry of such systems on the flow characteristics of their components and thus on the course of this phenomenon. From this point of view, the advantage of the methods presented in the paper is the development of a quick practical way for determining the pressure wave speed characterizing the individual pipelines comprising the analyzed flow system.

2. Laboratory Stand

One of the most important elements of the work presented in this paper is laboratory tests carried out on a test stand built in the laboratory hall of the Institute of Fluid-Flow Machinery of Polish Academy of Sciences in Gdansk—Figure 1. The stand consists of two copper pipes connected in series with the following geometric parameters:

- Pipe #1: inner diameter $D_1 = 20$ mm, wall thickness $e_1 = 1$ mm, length $L_1 = 49.3$ m
- Pipe #2: inner diameter $D_2 = 16$ mm, wall thickness $e_2 = 1$ mm, length $L_2 = 58.9$ m

The change in diameter between the pipes is stepwise.

The pipeline system is supplied from the upstream tank (horizontally arranged cylindrical pressure tank with a diameter of 2 m and total volume equal to 10 m^3 , with an air cushion). The maximum pressure in the upstream tank that could be maintained during the tests was 1.2 MPa of absolute pressure.

Water from the pipeline is directed to the downstream tank (tank opened to an atmosphere of total volume equal 8 m^3 : cube shape with side 2 m). The water in the stand flows in a closed circuit—it is pumped from the downstream tank by a pump unit equipped with a variable rotational speed drive through auxiliary pipelines to the upstream tank. From the upstream tank, it flows through the measuring pipeline system and auxiliary pipelines, which, together with the installed control fittings, are used to stabilize the initial conditions during the tests (pressure and flow in the measuring pipeline system).

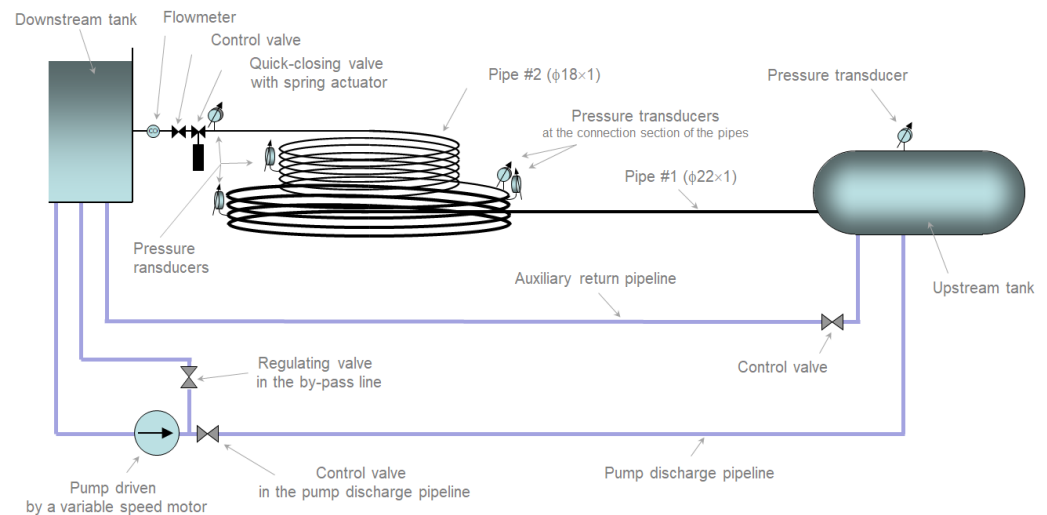


Figure 1. Laboratory stand for testing water hammers in series-connected pipes of different diameters.

At the end of the measuring pipeline (looking in the direction of water flow, i.e., at the end of pipe #2), a quick-closing ball valve is installed, which enables an almost stepwise shut-off of the water flow. A high degree of repeatability of the valve closing processes was achieved using a special spring drive. In the tested cases, the closing time, T_c , was close to 2 ms.

The laboratory stand is equipped with six pressure transducers installed in the initial, middle and end sections of each pipe, looking in the direction of the initial flow, and in the upstream tank. This paper focuses on the results measured at the valve (end of the pipe #2) because this is where the water hammer is most intense [19,46].

Each of the pressure transducers produced by KELLER Druckmesstechnik AG (Winterthur, Switzerland) was mounted on the pipeline with the use of a short (approx. 0.07 m) flexible impulse tube, which allows for significantly reducing the influence of pipeline structure vibrations on the measured pressure signal. The small length of the impulse tubes in relation to the total length of the pipeline and very high relative stiffness of their material (approx. 10 times higher than the coating of the measuring pipeline) minimized their influence on the measured pressure changes during the tested phenomenon.

The pressure transducers of the frequency band equal (0–2) kHz and the accuracy class: $\pm 0.1\%$ were used to measure the absolute pressure within the range of (0–4) MPa abs. The transducers characteristics were checked before the tests and immediately after their completion. It was estimated (according to [47]) that the uncertainty of the pressure measurements was ca. 0.47 m wc (meters of water column).

A turbine flow meter (manufacturer: Turbines Inc. (Altus, OK, USA), type: HA) with measurement inaccuracy (maximum measurement error) of 0.25% of the measured flow rate in the range (0.5–10) m/s and 1% in the range (0.1–0.5) m/s was used to measure the flow. The flowmeter indications were checked before and after the tests using the volumetric method.

The degree of opening of the quick-closing ball valve was monitored with a single-turn potentiometer. Before the tests, the potentiometer readings were calibrated with the appropriate valve positions: potentiometer signal readings for a fully closed valve position was defined as 0% of opening and respectively the signal for a fully opened valve was defined as 100% of its opening. The valve closing time was determined based on the closing course recorded in the data acquisition system. The uncertainty in determining this time is negligibly small and depends on the resolution of the potentiometer and the resolution of data recording.

A 16-bit measurement card and an application based on the DASYLab software (v.2016) by DASYTEC System Daten Technik GmbH (Ludwigsburg, Germany) were used to record the measurement data. Measurement signals were recorded with a frequency of 20 kHz.

The choice of such a high recording frequency opens the possibility of conducting future analyses of phenomena revealing themselves in the high frequency range (e.g., FSI). For the analysis, these signals were processed and the frequency was reduced to 1 kHz. This significantly facilitated the work related to data processing and therefore made it sufficient to conduct a reliable analysis of the phenomenon in terms of the set goals of the work being carried out.

Before the tests, the stand was carefully sluiced and filled with fresh tap water and left idle for five days in order to minimize the influence of the air contained in the water on the tested phenomenon. During the standstill, the system was kept open—valves in the pipeline lines open, pressures between the upstream tank and downstream tank equalized.

The measurement results for four selected test runs of a water hammer are shown in Figure 2. It presents pressure changes in the cross-section closest to the quick-closing valve (Figure 1). These pressure changes were recorded at different water pressures in the upstream tank (from 26.4 m wc to 119 m wc) and for different initial flows (from ca. 114 L/h to ca. 530 L/h). The compilation of these pressure waves allows the comparison of the influence of the initial conditions on the scope and nature of the recorded pressure changes during the water hammer.

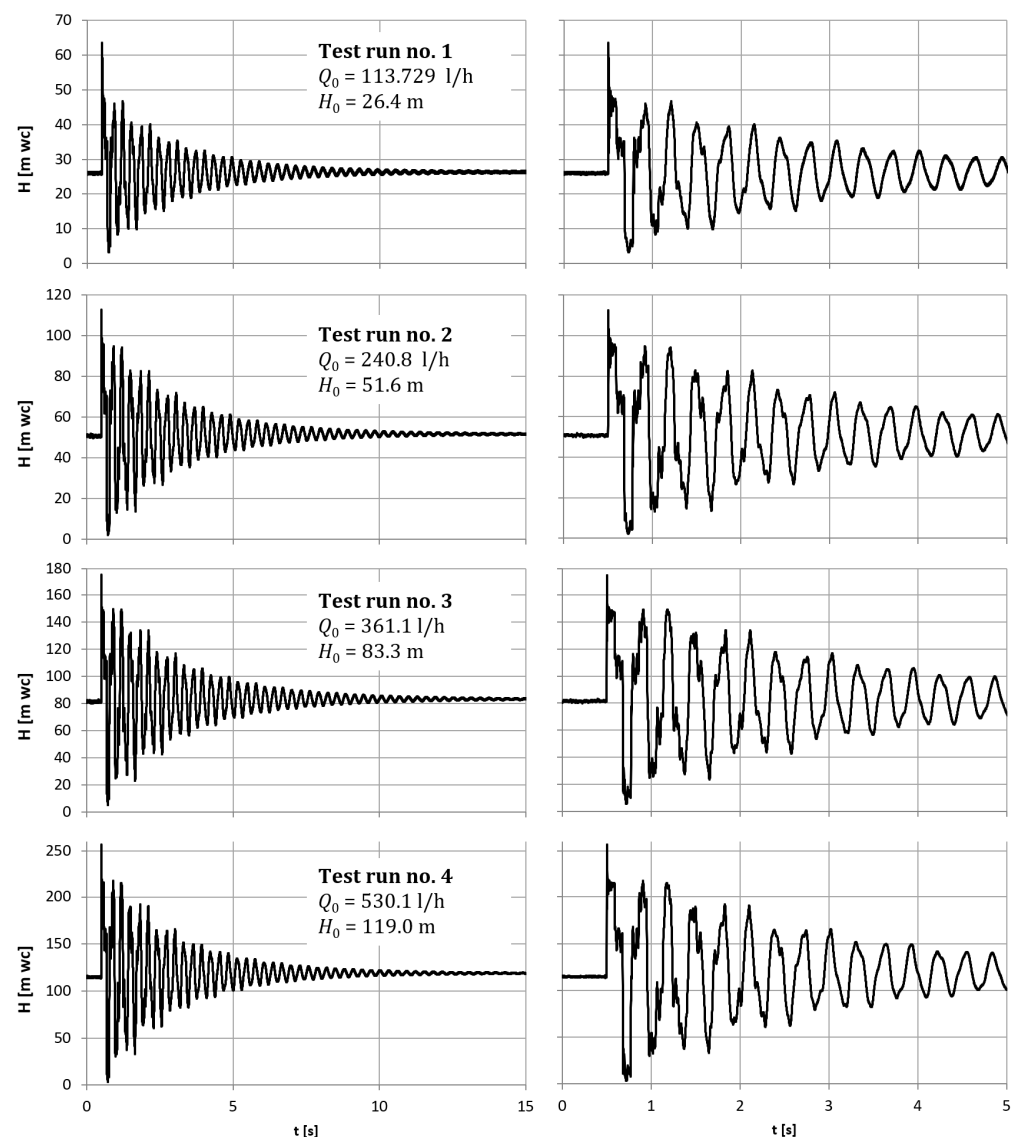


Figure 2. Examples of pressure changes measured at the valve for various initial conditions (pressure in the upstream tank, H_0 , and initial flow, Q_0).

There is a phenomenon of interference of these waves, which can be observed in the irregular wave shape, manifested by an asymmetric course with numerous refractions, particularly at the beginning of the course, covering from a few to a dozen consecutive amplitudes (ca. the first 7 s for each analyzed pressure course). The influence of the particular geometry of the hydraulic pipeline system on the course of pressure changes is clearly visible at about halfway through the first pressure peak where a decrease in the mean pressure level is observed—Figure 3. This is mainly the result of the passage of the pressure wave from the pipe with a smaller diameter (pipe #2 with the quick-closing valve installed at its end) to the pipe with a larger diameter (pipe #1). In the cross-section of the diameter change, the pressure wave is reflected propagating simultaneously in both pipes.

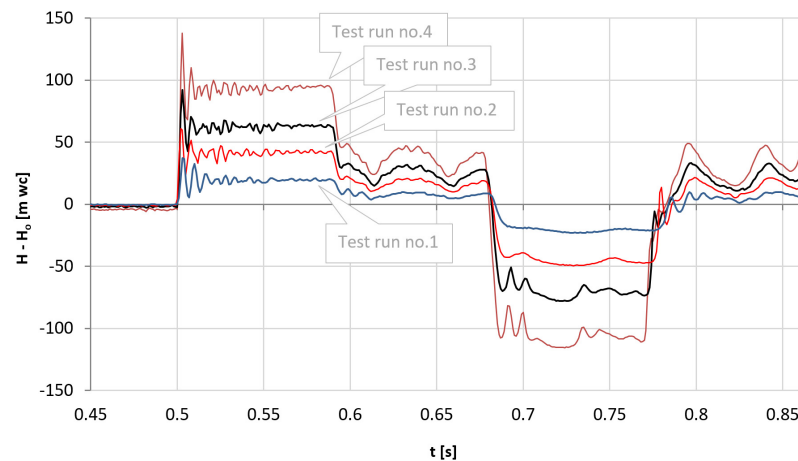


Figure 3. Comparison of the first period of the pressure wave for the analyzed water hammer test runs.

Pressure fluctuations, both high-frequency, accompanying mainly the first pressure increase, and low-frequency, observed e.g., between ~ 0.6 s and ~ 0.7 s, superimposed on the main water hammer pressure changes, may be related to various factors. Among the most important, apart from the geometric conditions of the pipeline (step change in diameter between two pipes), phenomena related to the impact of waves propagating in the liquid and in the material of the pipeline structure (FSI phenomenon [12]), as well as the impact of pipeline fastenings or the presence of air in the liquid, should be mentioned. The last two factors are manifested by relatively low frequency pressure changes (comparable to the main pressure changes related to the water hammer). The high-frequency pressure changes observed mainly at the beginning of the test runs are most likely related to the movement of the shut-off valve, which stops by hitting the bumper at high speed. This impact generates vibrations propagating in the structure of the valve and transferring to the structure of the pipeline. As a result, FSI occurs and a pressure wave superimposed on the main pressure changes is observed. However, the authors' experience shows that the applied impulse tubes and the mounting of the transducer, regardless of the construction of the pipeline, significantly reduces the impact of this phenomenon on the measured pressure signal in relation to the situation in which the transducers would be installed directly on the pipe wall.

The experimental tests were carried out in conditions which, due to the initial assumptions, were considered to have no significant impact on the main goal of the work, i.e., the development of a method for reliable determination of the pressure wave propagation speed in individual pipes and experimental verification of unsteady friction models used to simulate the phenomenon of a water hammer in complex piping systems. The obtained results presented in the later part of the paper confirmed the validity of these assumptions.

3. Determining the Pressure Wave Speed in the Tested System

In order to perform calculations on the water hammer in the analyzed flow system, it is necessary to know the pressure wave propagation speed in individual pipes of different diameters. One of the possible ways of determining this speed in the tested cases is based on the use of Joukowsky's theory [48], which links the first pressure amplitude (maximum increase) with the initial flow velocity and the pressure wave speed:

$$\Delta H_1 = \frac{a \cdot V_0}{g} = \frac{4a \cdot Q_0}{g \cdot \pi D^2} \quad (2)$$

where ΔH_1 is the first pressure amplitude [m wc] ($\Delta H_1 = H_1 - H_{init}$), H_1 is the pressure head of the first pressure rise caused by the water hammer [m wc], H_{init} is the pressure head in the initial steady-state condition before the water hammer [m wc], V_0 is the initial mean flow velocity [m/s], Q_0 is the initial volumetric flow [m³/s] and a is the pressure wave speed [m/s].

Formula (2) is correct for cases where the cut-off of the liquid flow in the pipeline takes place during time T_c , which is not longer than the time of the pressure wave circulating forth and back along the pipeline where the quick-closing valve is installed, i.e., in the time equal to half of the period T of the pressure wave in this pipeline:

$$T_c \leq \frac{T}{2} \rightarrow T_c \leq \frac{2L}{a} \quad (3)$$

where T is the pressure wave period [s] ($T = 4L/a$) and L is the length of pipeline [m].

For the analyzed laboratory system, condition Equation (3) is met: the valve closing time T_c is about 50 times shorter than the ratio $2L/a$ for pipeline #2. Therefore, the analysis of the uncertainty of determining the valve closing time, which is very small depending on resolution of potentiometer and data acquisition, is insignificant in relation to the analysis conducted in this paper.

The main problem with this method is that it requires knowing the exact values of Q_0 and ΔH_1 to be able to accurately determine the wave speed a using Equation (2). As shown in Figure 3, due to high frequency pressure oscillations, the most probable result of the unfavorable effect of vibrations in the structure caused by the abrupt closing of the shut-off valve, it is not possible to determine the value of ΔH_1 with the required precision. Additionally, the determination of the initial flow may be subject to a significant error resulting from the accuracy class of the flow measurement transducer used. Therefore, this paper proposes a method for determining the speed of pressure wave propagation based on the measurement of the timing of the passage of the pressure wave between two cross-sections in which pressure changes were measured during the tests.

In the later part of the paper, the second method is presented, which uses the frequency of free pressure oscillations measured in the final phase of their damping in the tested pipeline system to determine the speed of the pressure wave. This method was also applied to the analyzed cases of water hammer.

3.1. Method #1

Equipping the laboratory stand with pressure measurements in several cross-sections of the measuring pipeline opened the possibility of determining the speed of pressure wave propagation in the system using the measurement of time of the pressure wave passage between two sections in which the pressure measurements were carried out. After detailed analyses of the measurement signals, it was decided to use for this purpose the measurement signals from the transducer installed directly at the valve (transducer no. 1) and the transducer installed in about half of the pipe #2 (transducer no. 2)—Figure 1. In the case of the other signals, there was too high signal distortion manifested by pressure fluctuations originating mainly from wave reflections from the cross-section of diameter changes, but also from FSI effects, prevented their use in this method. Due to the fact that

as the water hammer phenomenon continues, these distortions also become present in the signals from transducers no. 1 and 2, the analysis could be carried out only for the first pressure increase after closing the valve—Figure 4.

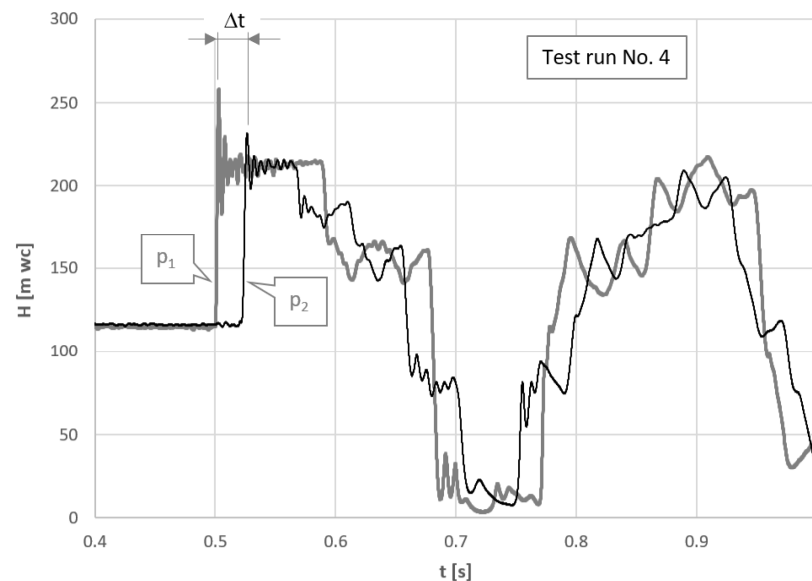


Figure 4. Pressure measurement signals in two measured sections of pipe #2: p_1 —pressure measurement at the valve; p_2 —pressure measurement in about half of pipe #2.

The distance between Sections 1 and 2 of the pressure measurement was $\Delta l = 29.392$ m. Using the following basic relationship:

$$a = \frac{\Delta l}{\Delta t} \quad (4)$$

the value of the pressure wave propagation speed in the pipe #2 $a = a_{2_meas}$ can be determined on the basis of the value Δt standing for the time of wave passage between the measurement sections.

To estimate the pressure wave speed in pipe #1 (a_{1_est}), which is connected to the upstream tank, the value of the pressure wave speed in pipe #2 (a_{2_meas}) can be used, determined on the basis of the analysis shown in Figure 4. For this purpose, the following formula can be used:

$$\frac{a_{1_est}}{a_{2_meas}} = \sqrt{\left(1 + \frac{D_2}{e_2} \cdot \frac{K}{E_2} c_{1,2}\right) / \left(1 + \frac{D_1}{e_1} \cdot \frac{K}{E_1} c_{1,1}\right)} \quad (5)$$

Formula (5) is based on Equation (1) and takes into account the fact that the pipelines used during the tests are made of the same material (copper) and are supported in the same way, and the underlying assumptions should be considered justified. For the considered case the pipe #1 ($D_1 = 0.02$ m, $e_1 = 0.001$ m) and pipe #2 ($D_2 = 0.016$ m, $e_2 = 0.001$ m) are made of the same material ($E_1 = E_2 = E = 120 \cdot 10^9$ for copper) and are rigidly fixed to the foundation in a similar way ($c_{1,1} = c_{1,2} = c_1 = 1 - \nu^2$ is equal 0.8775 using Poisson's ratio for copper pipes $\nu = 0.35$). The wave speed ratio defined by formula (5), calculated for $K = K_{water} = 2.21 \cdot 10^9$ Pa (at water at 23 °C and under pressure approx. 100 m wc [49]), is ca. 0.975.

In Table 1, the values of the pressure wave speed determined using Equations (4) and (5) are shown for both pipes of the measuring system. These values apply to four test runs differing in initial conditions (values of Q_0 and H_0). The uncertainty of these quantities is mainly related to the time resolution of the recorded pressure oscillations. Therefore, the relative uncertainty will depend on the time interval that is being measured. In the

analyzed cases, the time of the pressure wave passage between two measurement sections reaches values on the order of 10^{-2} s. Taking into account the recording frequency of measurement signals (20 kHz), this means that estimated relative uncertainty of measuring a_{1_est} and a_{2_meas} resulting from the procedure based on Equations (4) and (5) does not exceed 0.2% (the uncertainty of measuring the distance Δl between the transducers, which is estimated at about 0.015%, was omitted).

Table 1. Parameters of selected test runs with pressure wave speed determined using method #1.

Test No	Pressure in the Upstream Tank	Initial Flow	Time of Wave Passage between the Measurement Sections of Pipe #2 Spaced $\Delta l = 29.392$ m Apart	The Pressure Wave Speed in the Pipe #2 Determined on the Basis of Equation (4)	The Pressure Wave Speed in the Pipe #1 Calculated on the Basis of Equation (5)
	H_0		Δt	a_{2_meas}	a_{1_est}
-	m wc	L/h	ms	m/s	m/s
1	26.4	113.7	24.05	1222	1192
2	51.6	240.8	23.77	1236	1206
3	83.3	361.1	23.67	1242	1211
4	119.0	530.1	23.49	1251	1221

From all of the results presented in Table 1, attention is drawn to their quite clear dependence on the pressure in the upstream tank, H_0 , which indicates that higher speed of pressure wave propagation relates to the runs carried out at higher levels of this pressure. The most likely cause of this effect is discussed later in the paper.

3.2. Method #2

The direct effect of the configuration of the hydraulic pipeline system is the resultant frequency of pressure oscillations (free vibrations) observed at the end of the transient phenomenon—Figure 5. Based on the analysis of the pressure wave period for this phase of the phenomenon (averaged value from 20 selected final cycles of pressure oscillation in its developed phase, for which the impact of the change in diameter is insignificant and their shape is much more regular than for oscillations in the initial phase of the water hammer), the resultant wave speed a_{r_meas} was determined and its values are summarized in Table 2.

Table 2. Parameters of selected measurement runs tested on a laboratory stand together with data for determining the resultant pressure wave speed of the pipeline composed of two pipes with different diameters.

Test No	Pressure in the Upstream Tank	Initial Flow	Period of the Pressure Wave (Calculated from 20 Final Periods of Pressure Oscillations)	The Resultant Pressure Wave Speed in the Pipeline System Composed of 2 Pipes with Different Diameters
	H_0		T	a_{r_meas}
-	m wc	L/h	s	m/s
1	26.4	113.7	0.3120	1387
2	51.6	240.8	0.3090	1400
3	83.3	361.1	0.3065	1411
4	119.0	530.1	0.3043	1422

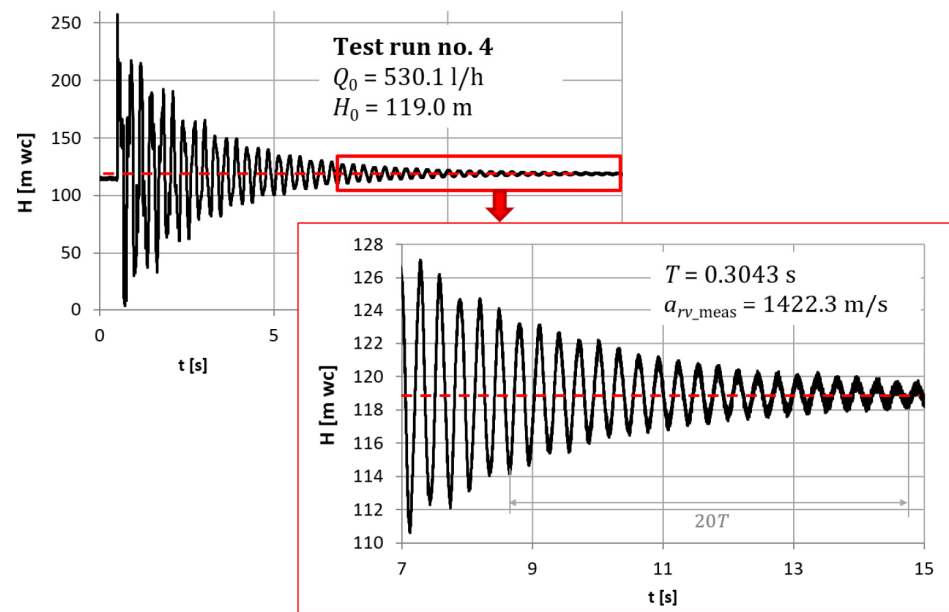


Figure 5. The method #2 of determining the resultant speed of the pressure wave (a_{r_meas}) in a system composed of two pipes of different diameters.

The comparison of the results summarized in Tables 1 and 2 and presented in Figure 6 shows that the determined resultant wave speed a_{r_meas} , similarly to the speed in individual sections determined using method #1, also depends on the level of equilibrium pressure (pressure in the upstream tank), H_0 . This effect is widely known and has been repeatedly confirmed in scientific research (e.g., in [46]). It results from the fact that in the liquid (in this case, water) there is a certain volume of air undissolved in it, mainly in the form of microbubbles. This volume, although usually small, can be responsible for a significant change in the bulk modulus as well as the density of the water–air fluid. Both of these quantities affect the speed of pressure wave propagation, reducing it in relation to the speed in the liquid without air. Moreover, due to the considerable compressibility of air, a change in the pressure of the fluid causes a change in the proportion of the volume of air to the volume of the liquid. This translates into changes in the bulk modulus and density of the fluid, which in turn causes changes in the propagation speed of the pressure wave under these conditions (i.e., greater pressure reduces the volume of air microbubbles in the fluid, which increases the propagation speed of the pressure wave). It is roughly estimated that in the analyzed cases the air content could be less than $10^{-3}\%$ of the total fluid volume at standard pressure [46].

It is noteworthy that the resultant wave speed, a_{r_meas} , is 7–10% higher than the speed value a_{2_meas} and by as much as 10–13% from a_{1_est} determined using Equations (4) and (5), respectively (method #1). Moreover, the value of a_{r_meas} is only 4–7% less than the speed of sound in water (1487.4 m/s under the test conditions).

The determination of the value of a_{r_meas} is burdened with a comparable absolute uncertainty as for the determination of a_{1_est} and a_{2_meas} using Equations (4) and (5). This is because in the case of determining the wave speed a_{r_meas} using method #2, the relative uncertainty does not depend only on the number of free oscillations that will be taken into account when determining the average period of the pressure wave. It must also take into account the change in the wave frequency during the phenomenon.

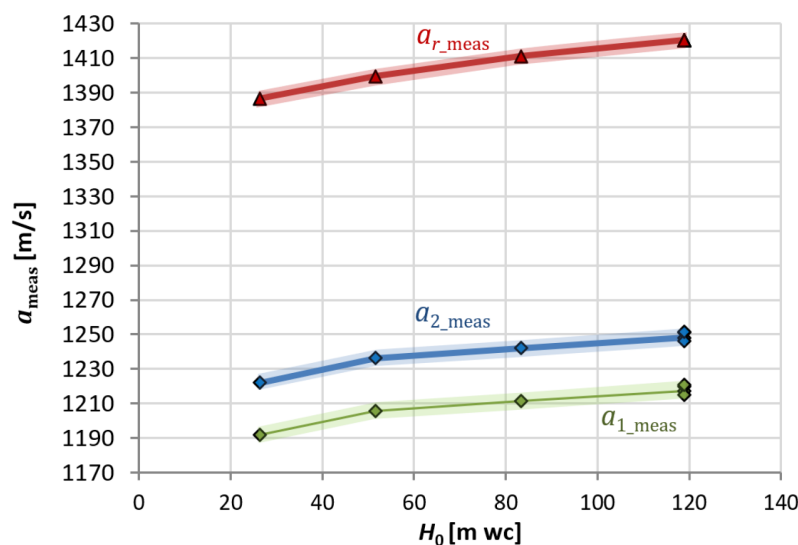


Figure 6. Pressure wave speed for pipe #1 and #2 (a_{1_est} , a_{2_meas}) determined using method #1 (based on the measurement of the time of pressure wave passage between two consecutive pipe cross-sections) and the speed (a_{r_meas}) of the resultant pressure wave (in the developed phase of oscillations).

It is known that friction causes a decrease in the wave frequency as the transient state phenomenon continues. Appendix A presents a rough analysis of the effect of damping on the wave frequency change—the analysis was carried out assuming a linear damping decrement and showed a negligible, approx. 0.05%, impact of such damping on reducing the frequency of linearly damped vibrations relative to undamped vibrations. In the case of a water hammer, friction is non-linear, which means that the frequency of the pressure wave during this phenomenon, and thus also the speed of pressure wave propagation, depends on its duration. In order to estimate this effect, method #2 was used based on the measurement of the time for six subsequent five-wave period time intervals. Additionally, the pressure wave speeds determined on this basis were compared with the value determined for 30 wave periods. The results presented in Figure 7 confirm the decrease in the speed of pressure wave propagation with the duration of the phenomenon. However, one should be careful in interpreting these results due to the observed scattering of the speed values around the trend line. This may be related to the fact that in the analyzed phase of the pressure oscillations, the influence of changes in the diameter of pipes in the flow system on the course of pressure changes can be still present. Nevertheless, it should be emphasized that this scattering is small (reaching a maximum of 2.5 m/s, i.e., approx. 0.15% of the average value) and confirms that the use of method #2 based on the average frequency value from several dozen periods of the pressure wave in its final phase does not significantly affect the results of this method. This should be taken into account when determining the uncertainty of the method, which should be about 0.2% for the analyzed cases, i.e., as for method #1.

The appropriate uncertainty band of method #1 determined in accordance with [47], together with the uncertainty band of method #2, were assessed based on the above considerations and are shown in Figure 6.

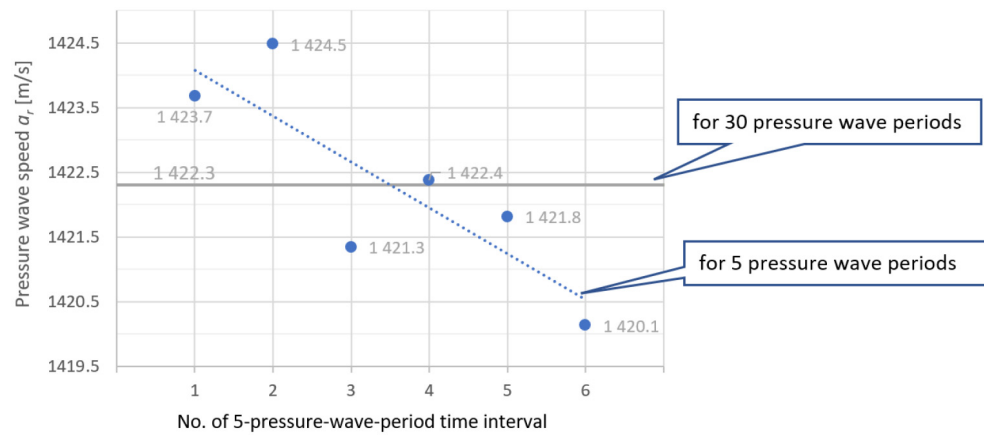


Figure 7. Comparison of the pressure wave propagation speed measured from the final phase of the water hammer using the time duration of 30 wave periods and 6 consecutive 5-wave periods.

The quantity a_{r_meas} can be used to determine the speed of pressure wave propagation in individual sections of the pipeline. This requires the assumption that this value corresponds to the value of the propagation speed, a_e , which would characterize a simple hydraulic system, composed of a uniform pipeline with equivalent, constant geometric (diameter, wall thickness) and material parameters (uniform along the entire length) equivalent to the real system according to the water hammer analysis. The approach based on replacing real systems built from a series of pipes with equivalent pipeline is very common in practice, especially in issues related to extensive transmission networks, where it is desirable to quickly and reliably estimate the effects of a water hammer. In the literature such a simplified analysis is recommended to be carried out, maintaining the similarity of inertia and friction forces and the time period of the pressure wave transition [19,20,23]. According to this principle, the pressure wave speed in the equivalent pipeline, a_e , (resulting from the assumption that the wave time period is preserved in each individual sections) is a function dependent on the geometrical parameters (length, cross-sectional area) and on the pressure wave speed in the individual i -th pipeline section. The assumption $a_e = a_{r_meas}$ and the knowledge of the full geometry of the real system, opens a chance to determine the value of the pressure wave speed in individual pipes included in a complex pipeline system. The validity of the results obtained with this procedure depends on the equivalent pipeline model used, as is shown below. One of the proposals of such a model is based on the following relationship [19,23]:

$$a_e = \frac{\sum L_i}{\sum L_i/a_i} \tag{6}$$

In this model, the speed a_e has an intermediate value between the values a_i for individual pipes of the pipeline system. However, such a result, assuming that the value of a_e should well approximate the value of the speed a_{r_meas} of the resultant pressure wave, is inconsistent with the results of the experiment presented in Tables 1 and 2 and in Figure 6. Therefore, in further calculations, based on [33,34], an alternative method of determining the equivalent speed in the pipeline system consisting of different pipes connected in series was used.

In accordance with this method, the value of a_e can be calculated using the Laplace transform-based linear analysis of the system built with series-connected pipes. The relationship that emerges from this analysis is as follows:

$$\frac{4L_e}{a_e} = \frac{2\pi}{\omega_e} \rightarrow a_e = \frac{2}{\pi} L_e \omega_e \tag{7}$$

where ω_e is the circular frequency of pressure oscillation (index e stands for “equivalent system”):

$$\omega_e = \frac{2\pi}{T_e}, \tag{8}$$

which in the case of two pipes connected in series fulfills the following equation [33,34]:

$$\frac{a_1 A_2}{a_2 A_1} \cdot \tan \frac{\omega_e L_1}{a_1} \cdot \tan \frac{\omega_e L_2}{a_2} = 1 \tag{9}$$

Other symbols in Equations (7)–(9) stand for: a_1 or a_2 is the actual pressure wave speed characteristic for each individual pipe [m/s]; A_1 or A_2 is the area of cross-section of each individual pipe [m²] ($A = 0.25 \pi \cdot D^2$); L_1 or L_2 is the length of the individual pipe [m]; L_e is the equivalent length of a series connected pipe system, being the sum of the lengths of the system components [m]; and T_e is the wave period [s].

It should be emphasized that the above analysis does not take into account the full impact of friction losses on the parameters of water hammer. Omitting the so-called unit resistance of the pipe does not mean that the losses are completely excluded from the analysis, but only their impact is reduced, which is manifested, inter alia, in a wave frequency change. However, as it is shown in the further analysis, such an assumption has a negligible effect on the wave speed in the tested system.

When the values of a_1 and a_2 are known, the Equation (9) enables the determination of the value of ω_e , and consequently, the value of the equivalent wave propagation speed, a_e .

On the other hand, with the known geometric parameters of the pipes, i.e., A_1 , A_2 and L_1 and L_2 , and the ratio a_1/a_2 given by Equation (5), the above procedure can be used to determine numerically the value of the pressure propagation speed in individual sections of the pipeline a_1 and a_2 in accordance with Equation (9) for a given value of ω_e .

The values of the pressure wave speed in individual pipes in the pipeline system, calculated in accordance with the described procedure for the analyzed test runs are presented in Table 3. These values were compared with the values of the pressure wave speed in individual pipes determined using method #1 based on Equations (4) and (5). The differences between the compared values are on average approx. 0.08% and max. 0.1% (this is within the uncertainty bands estimated for method #1 and #2). The comparison of the results obtained with the two analyzed methods confirms the positive verification of method #2.

Table 3. Values of pressure wave speed in the pipeline system—comparison of the values obtained using method #1 and method #2.

Test No	The Velocity of Propagation of the Resulting Pressure Wave in a System of 2 Pipelines with Variable Diameters, Calculated on the Basis of 20 Final Periods of Pressure Fluctuations	Pressure Wave Speed in Individual Pipes				Differences between the Values of Pressure Wave Propagation Velocity in Sections of the Pipeline Calculated on the Basis of Equation (9) and Determined on the Basis of Equation (4)
		Determined Using Method #1 (on the Basis of Equations (4) and (5))		Calculated Using Method #2 (for a_{r_meas} Basing on Equations (9) and (5))		
		Pipe #1	Pipe #2	Pipe #1	Pipe #2	
	a_{r_meas}	a_{1_est}	a_{2_meas}	a_1	a_2	$\frac{\Delta a_i}{a_{r_meas}}$
-	m/s	m/s	m/s	m/s	m/s	%
1	1387	1192	1222	1192	1223	0.07%
2	1400	1206	1236	1204	1234	−0.15%
3	1411	1211	1242	1213	1244	0.18%
4	1422	1221	1251	1223	1254	0.19%

It should be noted that in this method, unlike method #1, it is sufficient to know the pressure changes in one measurement cross-section only, which makes method #2 much more attractive to use than method #1 in the context of analyzing and determining the

speed of pressure wave propagation in systems composed of pipes connected in series, at least when it comes to less complex flow systems consisting of a few pipelines connected in series.

4. Verification of Water Hammer Simulation Method in Pipeline Systems Composed of Pipes of Various Diameters Series-Connected

Numerical analysis of the water hammer phenomenon generated by a quick flow cut-off in a system of two pipes with different diameters connected in series was carried out with the use of our own computer program. The algorithm of this program is based on the method of characteristics and takes into account the unsteadiness of friction losses according to several available models. The program has been positively verified on the basis of numerous comparisons of its results with the results of experiments, also those conducted in the IMP laboratory [3,5,6,50]. The program uses a special solution domain discretization procedure, which effectively eliminates the negative influence of numerical damping on the calculation results by maintaining the CFL condition throughout the whole grid of characteristics [51]. Details concerning this procedure and a general description of the MOC are presented in the Appendix B. The consequence of using a special procedure of discretization of the solution domain is, apart from the lack of numerical damping (Figure A2), also the lack of sensitivity of the proposed numerical method to changes in the grid density. It is important, however, that in order to use in calculations the parameters of each of the series-connected pipes of the hydraulic system as close as possible to the set/actual parameters, a sufficiently dense numerical grid is required (it is important to obtain the required low difference between the actual/set value of a and a_{grid} used in the calculations—Appendix B).

The calculations of the pressure–time courses obtained using the developed numerical method were compared with the runs recorded during tests on the laboratory stand in order to check the convergence between them. This work focuses on the pressure changes in the courses occurring in the cross-section directly at the quick-closing valve. The calculations were made taking into account the quasi-steady (based on the Hagen–Poiseuille law and Colebrook–White formula) and unsteady models (efficient version of the Vardy and Brown model [52,53] and two versions of the Brunone et al. model [54,55]) of friction losses described in detail in Appendix B.

4.1. Verification of the Numerical Method Using the Quasi-Steady Friction Loss Model

The calculations performed to carry out the comparative analysis were made for run no. 4 (the initial conditions are presented in Table 1) and together with the measured pressure heads are shown in Figure 8.

Since the analysis of the pressure wave propagation speed determined by the method #1 and method #2 showed a high degree of their compatibility, the verification of calculations made using friction loss models was carried out for the results obtained with the method easier to use, i.e., the proposed method #2 (based on Equation (9)—Table 3): $a_1 = 1223$ m/s and $a_2 = 1254$ m/s for a pipe with a larger and smaller diameter, respectively.

The numerical grid used in the calculations (a regular, rectangular grid) had 446 nodes along the pipes x axis (206 for pipe No. 1 and 240 for pipe No. 2) and 76,642 nodes along the time axis (simulation time $t_{\text{max}} = 15$ s). Details regarding the method of discretization of the solution region are included in Appendix B. According to Figure A1, the grid within each pipeline is identical, but differs in the dimensions of the grid cells. The dimensions of the cells along the x -axis (pipelines axis), defined according to the relationship $\Delta x_i = \Delta t_i \cdot a_{i_grid}$, where a_{i_grid} is defined in Equation (A25), were as follows:

- For pipe #1: $\Delta x_1 = 0.2393$ m
- For pipe #2: $\Delta x_2 = 0.2454$ m

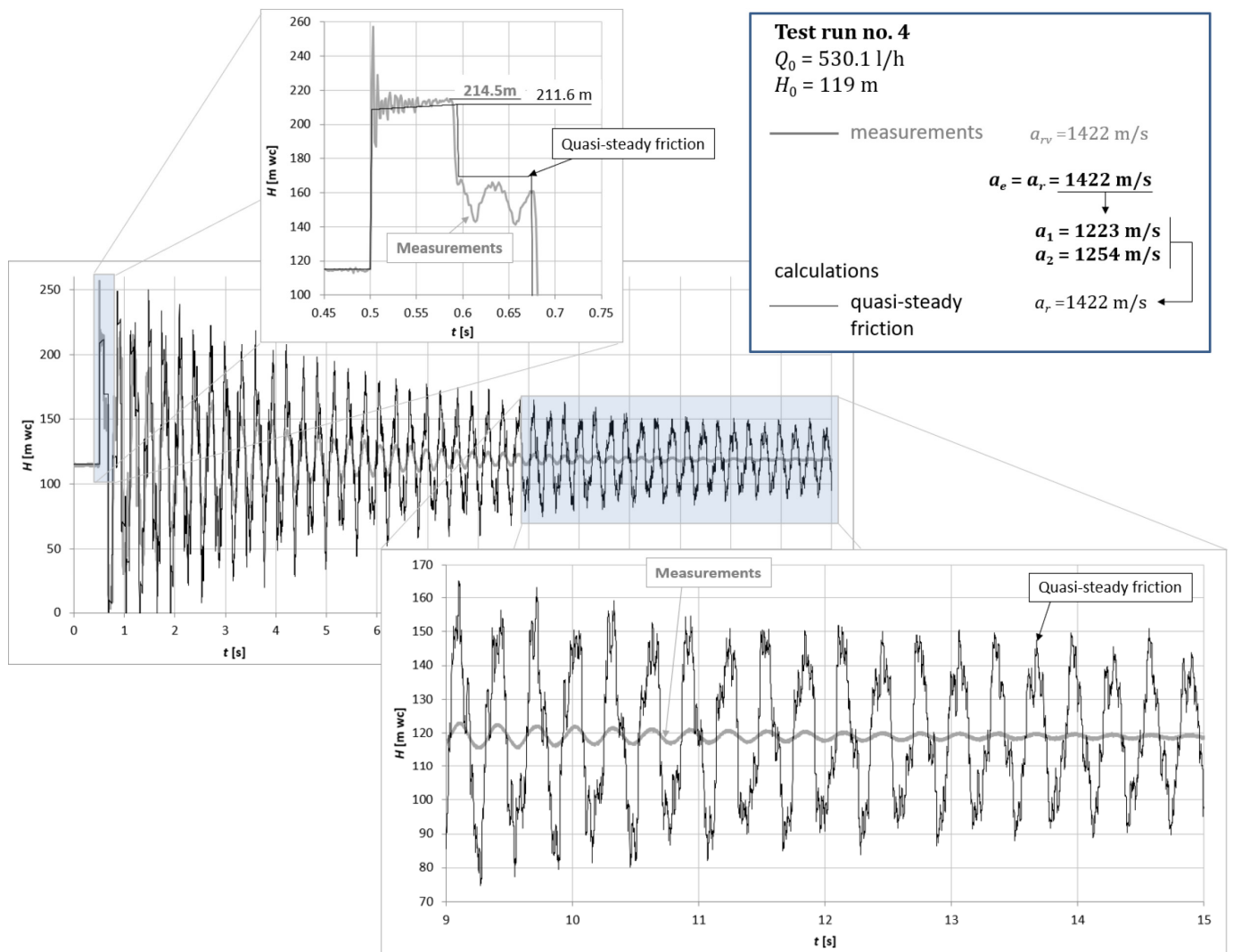


Figure 8. Comparison of the pressure oscillations measured at the valve (test No. 4) with the calculated pressure wave obtained with the use of the quasi-steady model of friction losses for the wave speed in pipes connected in series determined on the basis of Equation (9).

The grid dimensions along the t -axis for both pipelines ($\Delta t_1 = \Delta t_2 = \Delta t$) were equal $\Delta t = 1.957 \cdot 10^{-4}$ s. Thanks to such selection of grid size, the relative error of mapping the wave speed in individual pipes was $|\varepsilon_{a_1}| = 0.02\%$, $|\varepsilon_{a_2}| = 0.01\%$ for the respective pipes (Equation (A26) in Appendix B). It should be emphasized here that the relative errors of mapping the wave speed in individual pipes presented above do not generate numerical damping, but only affect the discrepancies between the set (a_i) and the calculated (a_{i_grid}) values of pressure wave propagation speed. The errors associated with this are not less than ten times smaller than the uncertainty of methods #1 and #2 of determining the speed a_i from the measurement data, so they do not have a significant impact on the calculation results and conclusions formulated at a later stage of the analysis.

In order to check the calculation algorithm, calculations were made using a quasi-steady model of friction losses (calculations carried out using the Hagen–Poiseuille law and the Colebrook–White formula were performed with the value of density $\rho = 998.97 \text{ kg/m}^3$ and dynamic viscosity $\mu = 0.938 \cdot 10^{-3} \text{ Pa}\cdot\text{s}$ for water at $23 \text{ }^\circ\text{C}$ and assuming the absolute roughness of the inner surface of the copper pipe $k_r = 2 \cdot 10^{-6} \text{ m}$ —see Equations (A11)–(A13) in Appendix B).

The comparison of the measurement and calculation results made with the use of the quasi-steady model of friction losses, presented in Figure 8, showed a lack of agreement

between them in terms of changes in pressure amplitudes over time and the shape of the pressure wave. Numerous wave reflections persisting throughout the simulated time are characteristic for the calculated pressure wave, while the measured wave shows a gentle, sinusoidal-like course in the developed phase of the pressure oscillation.

These observations confirm the commonly known features of the quasi-steady model of friction losses, which, apart from the first few pressure amplitudes, does not allow for an accurate simulation of the water hammer phenomenon. However, it should be noted that in the presented case the results of the calculations show a good agreement in regard to the value of the first pressure amplitude (excluding high-frequency pressure peaks)—the calculations show that the main pressure change from the water hammer (measured as shown in Figure 8) is underestimated by only about 1%.

However, it is noteworthy that the calculation results obtained using the quasi-steady friction model show a very good agreement with the frequencies of the measured pressure wave—the wave period that is determined on the basis of the developed phase of pressure oscillation is approx. 0.3043 s for both the measured and calculated pressure waves.

This confirms the correctness of the assumptions underlying the proposed method #2 of determining the value of the pressure wave speed in individual pipes based on the equivalent pipeline model described in [33].

4.2. Verification of the Numerical Method Using the Models of Unsteady Friction Losses

The main scope of this work was focused on the verification of unsteady friction models used to simulate the water hammer in the analyzed system consisting of pipes of different diameters connected in series. The expected better compliance of the pressure amplitudes between measurements and calculations with unsteady friction models has been validated for the efficient version of the Vardy and Brown model (Vardy and Brown efficient) as well as the Brunone et al. model in version 1 (with the k_3 coefficient calculated from Equation (A18)—Brunone et al. ver.1) and version 2 (with a constant value of k_3 coefficient adjusted to the reference run—in the case of the test run No. 4, the assumed value of this coefficient was $k_3 = 0.045$ —Brunone et al. ver. 2). These models were also subjected to experimental verification in the authors' previous studies for a homogeneous pipeline with constant parameters [3].

The results of the calculations for the above-described Vardy and Brown efficient and Brunone et al. ver. 1 models are shown in Figure 9. In terms of quality, the pressure wave simulated using the Vardy and Brown efficient model represents much better agreement with the measurements than the calculations carried out using the Brunone et al. ver. 1 model. The Vardy and Brown efficient model generates a wave that in the developed phase of oscillations is regular, very similar to the measured wave. In the case of the Brunone et al. ver. 1 model, the pressure wave is much more irregular, which indicates that the combination of pipes with a stepwise change in diameter affects the calculated pressure wave over the entire analyzed time of simulation. This means that the shape of this wave is significantly different from the reference wave (measured), especially in the developed phase of pressure oscillation. In addition, attention should be paid to a better compliance of the pressure wave simulated using the Vardy and Brown efficient model with the measurements mainly in terms of wave attenuation.

Comparison of the calculation results with the measurement results showed that the period of computational pressure wave, T , depending on the model used, is as follows:

- approx. 0.309 s for the Vardy and Brown efficient model,
- approx. 0.310 s for the Brunone et al. ver. 1 model.

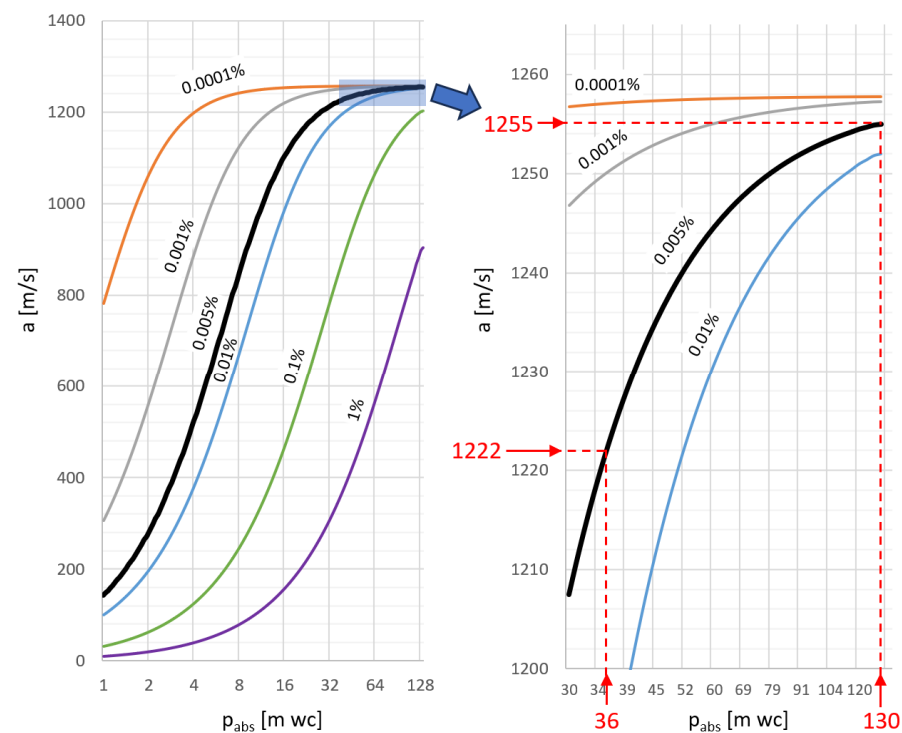


Figure 9. Analysis of the gas fraction content in the liquid during laboratory tests.

This means that the frequency of the wave simulated with the use of these models of friction losses is lower by almost 1.7% and 1.8%, respectively, than the frequency of the wave measured during the tests. The resultant wave speed a_r in the case of calculations was 1398 m/s for the Vardy and Brown efficient model and 1397 m/s for the Brunone et al. ver. 1 model. These values are less than the resultant speed value for the measured wave (1422 m/s). This discrepancy cannot be the result of pressure wave damping and its insignificant impact on the pressure wave frequency as was shown in the analysis presented in Figure 7 and in Appendix A. Taking into account the results of these analyses, it can be stated that the friction-induced damping effect of the pressure wave, because it is vanishingly small, cannot be considered the cause of the observed disagreement and it should be assumed that these differences most likely result from the properties of the models of friction losses used. However, confirmation of this thesis requires additional research and analyses. Nevertheless, it should be emphasized that there is a very high agreement with the measurements considering the damping ratio achieved using the Vardy and Brown efficient model and that the differences in the pressure wave propagation speed are relatively small. This means that this model, apart from its theoretical quality, seems to have great potential for application in engineering practice.

5. Discussion

The results of experimental tests presented in this paper, carried out on a stand equipped with a copper pipeline consisting of two pipes of different diameters connected in series, were subjected to detailed analyses. Thanks to two different methods of determining the pressure wave speed in the system from the experimental data, it has been shown, among others, that this quantity depends on the pressure level in the supply tank. The presence of an amount of gas (air) microbubbles in the water, which could not be completely eliminated before the tests, despite leaving the water at rest for several days, was considered the most probable cause of this.

The presence of undissolved air may introduce additional uncertainty in the results obtained using the proposed methods. This uncertainty can be minimized by conducting a detailed analysis of the effect of air content on the pressure wave speed according to the

methodology presented in [46] (chapter 8-2, pp. 139–142). It is based on the dependence of pressure wave speed changes on the pressure level and gas fraction content in the air–water mixture. This dependence results from taking into account the changes in the bulk modulus and density caused by the presence of air in water. This is reflected in the formula for the pressure wave speed, which, after some simplifying assumptions, shows its dependence on the pipeline geometry (D , e) and the Young's modulus of the pipeline material (E), as well as on the liquid (water) bulk modulus K , absolute pressure p_{abs} and the gas fraction content determined from the ratio of the gas volume to the total volume of the gas–water mixture V_g/V :

$$a = \sqrt{\frac{\frac{K}{\rho}}{1 + \frac{KD}{Ee} + \frac{V_g}{V} \frac{K}{p_{abs}}}} \quad (10)$$

The analysis carried out for different values of the V_g/V ratios is presented in Figure 9 and concerns changes in the pressure wave speed in pipeline #2. The changes in the pressure wave speed measured during the experiment using method #1 under the pressure conditions p_{abs} during the laboratory tests (from 36 m wc to 130 m wc) allowed for determining the gas fraction in the gas–water mixture at approx. $V_g/V = 0.005\%$.

As it results from the presented analysis, the air content in the laboratory conditions causes a change in the propagation speed by $\pm 1.3\%$. The range of these changes justifies the statement that the content of undissolved air in the water present in the laboratory conditions does not introduce significant uncertainty into the presented considerations.

The dependence of the pressure wave speed on the gas fraction in the fluid is shown in Figure 10. It is worth emphasizing that for high gas contents the change in wave velocity increases rapidly, but in the range up to $V_g/V = 0.15\%$, this change is not greater than 10%.

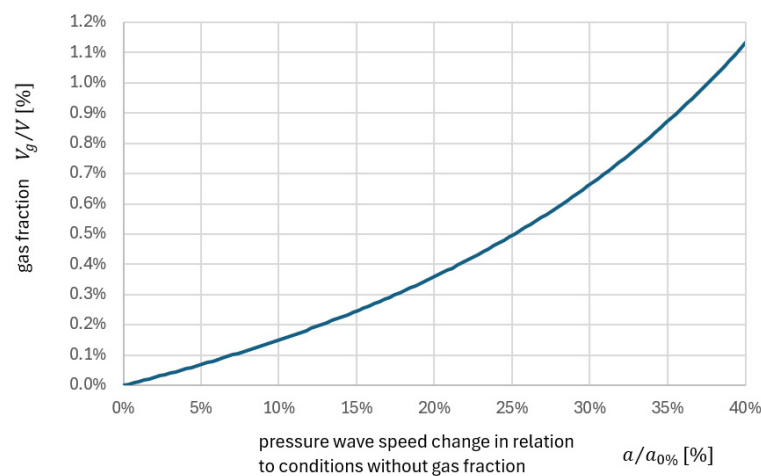


Figure 10. Pressure wave speed change in relation to gas fraction in the fluid.

It should be emphasized that the change in pressure wave speed with the change in gas volume, especially at low V_g/V , does not affect the uncertainty of the proposed methods because they are based on precise time measurements (method #1 determines the pressure wave speed based on the wave transit time between two pipeline cross-sections, while method #2 is based on the wave period in the free oscillation phase).

The test results show the relatively high frequency of free pressure oscillations (for a pipeline of full length $L = L_1 + L_2$) in the final (developed) phase of the water hammer. Its value in the cases tested on the stand was higher than the results from the theory of pressure wave propagation in individual pipes, without considering the process of their mutual interaction. This effect is not compatible with some equivalent models assuming that for systems composed of many pipes with different diameters and/or material characteristics, the equivalent pressure wave speed (equal to the resultant wave speed) follows from the

principle of maintaining the total wave transit time in individual pipes. This means that according to such models, the equivalent pressure wave speed should have an intermediate value between the speed values for individual serially-connected pipes. The conducted research presented in this paper showed that for the developed phase of the water hammer, these results were not confirmed—the measured resultant wave speed values for the final stage of the pressure course in the tested cases were significantly higher than wave speed values characteristics for each individual pipe.

The results of the calculations made using the method of characteristics with the special discretization procedure of the solution domain that allows to eliminate the numerical damping confirmed that for the laboratory test stand configuration the computational resultant pressure wave is also characterized by a wave speed exceeding each of the wave speeds calculated for the individual pipes.

This paper proposes a procedure for determining the pressure wave speed in individual pipes of a pipeline system on the basis of the resultant pressure wave speed read from the measurements and with the use of appropriate theoretical considerations regarding the equivalent model presented in [33,34]. The proposed method was verified on the basis of the results obtained using the method of determining the pressure wave propagation speed in individual pipes of the flow system, which uses the time of passage of the pressure wave between adjacent measurement sections. It has been shown that the uncertainties of both methods are comparable, while the proposed method requires only the knowledge of one course of pressure changes, which makes it attractive especially in terms of its practical use. Thanks to this procedure and the use of unsteady friction loss models, the numerical simulation method obtains results that are highly compatible with the measurement results.

This paper proposes two methods, the results of which are very similar. Method #2, which uses the measurement of the final phase of free pressure oscillations, is, however, easier to use from a practical point of view. This is because it allows for determining the pressure wave speed in individual pipelines of the flow system based on a single pressure measurement in any chosen cross-section of the flow system (the closer to the shut-off valve causing the water hammer the better, but this is not a necessary condition for this method). Method #1 requires measuring the pressure in two cross-sections of one pipeline, most preferably the pipeline in which the flow is cut off by a valve. While in practice flow systems are usually not equipped with conveniently installed measurement equipment, method #1 may be more problematic to use than method #2.

The increase in the complexity of the system construction increases the level of complexity when using the proposed methods for determining the wave velocity in individual pipeline elements. Method #2 can be used for systems consisting of a larger number of pipelines connected in series using the more general version of Equation (9) in the following form [33]:

$$\sum_{i=1}^{n-1} \left[\frac{a_i}{A_i} \cdot \tan \frac{\omega L_i}{a_i} \sum_{j=i+1}^n \left(\frac{A_j}{a_j} \cdot \tan \frac{\omega L_j}{a_j} \right) \right] = 1 \quad (11)$$

where n is the number of pipelines connected in series ($n > 1$) and i, j are the indices of the individual pipelines.

In the case of very complex flow systems, solving Equation (11) and determining the pressure wave speed for individual pipelines can be quite problematic. Therefore, in such a situation, using method #1 can be an effective alternative. However, it should be remembered that the condition for using this method is to perform two pressure measurements in appropriately spaced cross-sections of one pipeline.

Based on the results of verification analysis of the numerical method, it was shown that the calculation runs based on the unsteady models of friction losses show a high degree of compliance in the prediction of the damping rate of pressure waves, while discrepancies of several percent were found regarding the underestimation of the frequency of the simulated pressure wave in comparison with the one recorded during the laboratory tests. On the other hand, the use of the quasi-steady friction loss model showed a fairly

well-known inconsistency between the calculated and measured waveforms in terms of changes in pressure amplitudes over time and the shape of pressure waves, but almost perfect agreement was found between the frequencies of the measured wave and the waves calculated with the use of this model. Therefore, the thesis that the observed effect of a few percent reduction in the frequency of pressure waves simulated using unsteady models of friction losses results from the properties of these models is justified. This issue requires further work in order to improve the accuracy of the calculations obtained using unsteady models as regard to the frequency of the pressure waves.

6. Conclusions

The paper proposes methods for determining the pressure wave propagation speed in pipelines connected in series. The analyses carried out confirmed the reliability of the results obtained with their use. Due to the simplicity of the methods, they are convenient tools that can be successfully used in engineering practice to reliably predict the course of the water hammer phenomenon.

The additional aim of this work was to verify unsteady friction models based on the results of experimental tests carried out for an elastic pipeline system consisting of two series-connected pipes of different diameters. The experimentally verified numerical method (which does not generate numerical damping) together with the method of determining the pressure wave propagation speed (characterized by low uncertainty) from measurement data, allow for achieving conditions for objective evaluation of the analyzed friction models. The results of this work are a contribution to both the assessment of the friction modeling methods, as one of the most difficult issues in this area of research, as well as experimental studies of the phenomenon of a water hammer in complex hydraulic systems and practical aspects related to this phenomenon.

Research areas requiring further work indicated in this paper are important in the context of methods enabling the most accurate simulation of water hammers in real flow systems. Positive verification of such numerical methods will allow, *inter alia*, (1) reducing the uncertainty of estimating the immediate and fatigue strength of pressure systems, (2) preparing an appropriate design of flow systems, (3) taking into account the selection of appropriate fittings for regulating and cutting off the flow, and (4) actively controlling the water hammer phenomenon and protecting against its dangerous effects.

Author Contributions: Conceptualization, M.L. and A.A.; methodology, M.L. and A.A.; software, M.L.; validation, M.L.; formal analysis, M.L. and A.A.; investigation, M.L.; resources, M.L.; data curation, M.L.; writing—original draft preparation, M.L.; writing—review and editing, A.A.; visualization, M.L. All authors have read and agreed to the published version of the manuscript.

Funding: This research received no external funding.

Institutional Review Board Statement: Not applicable.

Informed Consent Statement: Not applicable.

Data Availability Statement: The data that support the findings of this study are available from the corresponding author upon reasonable request.

Acknowledgments: This research was carried out as part of the statutory work of the Szewalski Institute of Fluid-Flow Machinery of Polish Academy of Sciences.

Conflicts of Interest: The authors declare no conflicts of interest.

Appendix A. Analysis of the Impact of Pressure Wave Damping on the Wave Speed

In the above-mentioned two methods of determining the pressure wave speed in each of the pipes connected in series, the impact of wave damping was neglected or significantly reduced. Damping, according to the theory of vibrations, reduces their frequency. Treating pressure waves as damped vibrations, it is possible to estimate the impact of the damping ratio on the frequency reduction, *i.e.*, reduction of wave velocity [56,57].

The circular frequency of damped vibrations is determined from following formula:

$$\omega = \frac{2\pi}{T} \tag{A1}$$

Assuming that the pressure wave observed during the laboratory tests is an example of linearly damped vibrations, it can be assumed that the circular frequency of these vibrations is related to the circular frequency of undamped vibrations, ω_0 , according to the following relation:

$$\omega = \sqrt{\omega_0^2 - h^2} \tag{A2}$$

where h is the damping coefficient constituting the exponent of the function describing the change in time of the amplitude of linearly damped vibrations:

$$A(t) \propto e^{-ht} \tag{A3}$$

It follows from (8) and (A2) that the circular frequency of undamped vibrations can be determined as follows:

$$\omega_0 = \sqrt{\omega^2 + h^2} = \sqrt{\left(\frac{2\pi}{T}\right)^2 + h^2} \tag{A4}$$

The damping coefficient h in the exponent of the function (A3) can be defined as follows:

$$h = \delta \frac{2}{T} = \delta \frac{\omega}{\pi} \tag{A5}$$

The constant logarithmic damping decrement, δ , characteristic for this type of vibration, is defined as follows:

$$\delta = \ln \frac{|A_i|}{|A_{i+1}|} \tag{A6}$$

The presented definitions (A2)–(A6) show that the influence of damping on the circular frequency can be calculated as follows:

$$\omega_0 - \omega = \frac{2}{T} \left(\sqrt{\pi^2 + \ln^2 \frac{|A_i|}{|A_{i+1}|}} - \pi \right) \tag{A7}$$

An example analysis of the developed phase of the water hammer course presented in Figure 5 (main text of the paper) showed that the ratio of successive oscillation amplitudes is on average ~ 1.1 , which means that for the wave period $T = 0.3043$ s, the damping share in the circular frequency is:

$$\frac{\omega_0 - \omega}{\omega_0} \cong 0.05\% \tag{A8}$$

Appendix B. Numerical Method

The equations describing the water hammer phenomenon, which are used in this work, have the following form [19]:

- Continuity equation:

$$\frac{\partial H}{\partial t} + \frac{a^2}{g} \frac{\partial V}{\partial x} = 0 \tag{A9}$$

- Momentum equation:

$$\frac{\partial V}{\partial t} + g \frac{\partial H}{\partial x} + g \cdot J = 0 \tag{A10}$$

where:

V —flow velocity in the pipe [m/s];

H —pressure head [m wc];
 J —unit pressure losses [-];
 a —pressure wave speed [m/s];
 x —coordinate along the axis of the pipe [m];
 t —time coordinate [s];
 g —acceleration of gravity [m/s²].

The component of unit pressure losses can be represented using the Darcy–Weisbach formula:

$$J = f \frac{1}{D} \cdot \frac{V|V|}{2g} \quad (\text{A11})$$

where the friction coefficient, f , is defined depending on the friction loss model used in the calculation. The following models were used in this work:

- Quasi-steady model, in which the value of the coefficient f is calculated using:
 - Hagen–Poiseuille law for laminar flows $Re \leq 2320$ [58]:

$$f = \frac{64}{Re} \quad (\text{A12})$$

- Colebrook–White formula (Colebrook 1939) for transient and turbulent flow conditions $Re > 2320$:

$$\frac{1}{\sqrt{f}} = -2 \log \left(\frac{2.51}{Re \sqrt{f}} + \frac{k_r}{3.71D} \right) \quad (\text{A13})$$

where:

Re —Reynolds number: $Re = VD\rho/\mu$ [-];
 ρ —liquid density [kg·m⁻³];
 μ —dynamic viscosity coefficient [Pa·s];
 k_r —absolute roughness of the inner surface of the pipe [m];

- Unsteady friction models:
 - The Vardy and Brown model [52], in which the loss term is calculated based on the history of flow changes. The range of applications for this model includes smooth pipes and turbulent flows. The model has been positively verified by the authors in [3]. The efficient version of this model, prepared by Vítkovský et al. [53], which allows for a significant reduction in the requirements for computing, was considered in the calculations. According to this model, the unit friction loss term in equation (A11) has the following form:

$$J(t) = f \frac{1}{D} \cdot \frac{V(t)|V(t)|}{2g} + \frac{16\mu}{\rho g D^2} \int_0^t \frac{\partial V}{\partial t^*} W(t - t^*) dt^* \quad (\text{A14})$$

where:

W —weighting function defined in the domain of dimensionless time $\tau = 4\mu t / \rho D^2$ in the form:

$$W(\tau) = \frac{A^* e^{-B^* \tau}}{\sqrt{\tau}} \quad (\text{A15})$$

for:

$$\begin{aligned}
 A^* &= \frac{1}{2} \sqrt{\frac{\nu_w}{\pi \nu_{lam}}}, \\
 B^* &= \frac{Re^\kappa}{12.86}, \\
 \kappa &= \lg(15.29 \cdot Re^{-0.0567}),
 \end{aligned}$$

ν_w —kinematic viscosity at the wall of the pipeline [m²/s],

ν_{lam} —laminar kinematic viscosity [m^2/s].

In the proposal of Vitkovský et al., the weighting function W is approximated using the following expression:

$$W(\tau) \approx W_{app}(\tau) = \sum_{k=1}^N A^* m_k^* e^{-(n_k^* + B^*)\tau} \tag{A16}$$

where the coefficients m_k^* and n_k^* for $k = (1, 2, \dots, 10)$ take the values from Table A1:

Table A1. Values of coefficients for calculating the weighting function according to (A16).

k	1	2	3	4	5	6	7	8	9	10
m_k^*	5.03362	6.4876	10.7735	19.904	37.4754	70.7117	133.46	251.933	476.597	932.86
n_k^*	4.78793	51.0897	210.868	765.03	2731.01	9731.44	34,668.5	123,511	440,374	1,590,300

- In the model of Brunone et al. [54,55], the loss term is calculated on the basis of instantaneous flow velocity and flow acceleration values. According to this model, the unit friction loss term in Equation (A11) has the following form:

$$J(t) = f \frac{1}{D} \cdot \frac{V(t)|V(t)|}{2g} + \frac{k_3}{g} \left(\frac{\partial V}{\partial t} - a \frac{\partial V}{\partial x} \right) \tag{A17}$$

Two versions of this model were considered in the calculations:

- In the first (universal) version, the k_3 coefficient, which is the basic element of this model, is calculated from the formula proposed by Vardy and Brown [52], which makes its value dependent on the flow rate value:

$$k_3 = \left(2\sqrt{B^*} \right)^{-1} \tag{A18}$$

- In the second (the most popular) version, the value of the k_3 coefficient is selected in a way that guarantees the best possible adjustment of the calculation course to the measured course.

In the applied method of characteristics, the Equations (A9) and (A10) are transformed into a system of ordinary differential equations described on the lines of the characteristics C^+ and C^- , along which the disturbance in the liquid spreads:

$$\text{–For } C^+ : dV + \frac{g}{a} dH + gJ \cdot dt = 0 \tag{A19}$$

$$\text{–For } C^- : dV - \frac{g}{a} dH + gJ \cdot dt = 0 \tag{A20}$$

To integrate the system of Equations (A19) and (A20), the first-order finite difference approximation scheme is used:

$$\text{–For } C^+ : (V_P - V_A) + \frac{g}{a} (H_P - H_A) + (gJ)_A \cdot \Delta t = 0 \tag{A21}$$

$$\text{–For } C^- : (V_P - V_B) - \frac{g}{a} (H_P - H_B) + (gJ)_B \cdot \Delta t = 0 \tag{A22}$$

The characteristic lines are described by the following equations:

$$C^+ : \frac{dx}{dt} = a ; \tag{A23}$$

$$C^- : \frac{dx}{dt} = -a \tag{A24}$$

The applied method uses a rectangular grid—Figure A1. In order to ensure the stability of calculations without generating numerical attenuation, it is necessary to apply the solution domain discretization procedure, which ensures that the following condition is met [51]:

$$\frac{\Delta x}{\Delta t} = a \tag{A25}$$

This condition must be met for each i -th pipe of the analyzed pipeline system.

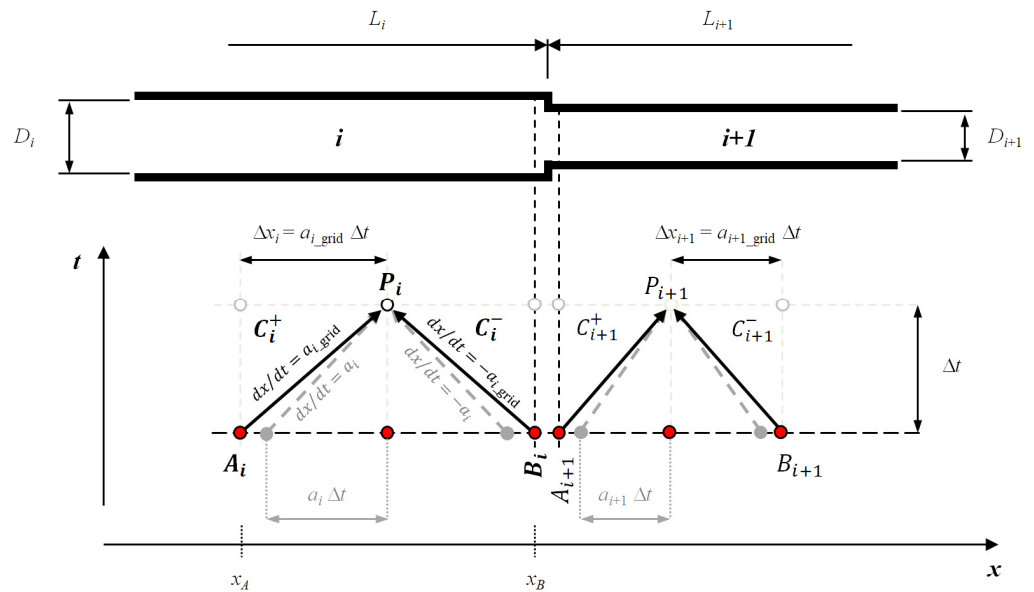


Figure A1. Discretization of the solution domain in the method of characteristics.

Discretization of the solution domain, which maintains the pipe geometry, requires that the lengths of the individual pipes be an integer multiple of the numerical step length, Δx , determined for these pipes in accordance with condition (A25). Moreover, in order to eliminate errors in the interpolation of the function values between the grid nodes, it is assumed that the simulation time step, Δt , is the same for all pipes connected in series:

$$L_i = m_i \cdot \Delta x_i = m_i \cdot a_i \Delta t \tag{A26}$$

The conditions (A25) and (A26) show the need for an appropriate adjustment of the numerical grid by correcting the value of the pressure wave speed in individual pipes, a_i . As a result of such a fit, new values of the pressure wave speed, a_{i_grid} , are determined for the grids belonging to each i -th analyzed pipes:

$$a_{i_grid} = a_i + \Delta a_i \tag{A27}$$

The appropriate values of Δx_i and Δt characterizing the grids are selected in such a way as to minimize the error defined by the following formula:

$$\varepsilon = \sum_{i=1}^n \frac{|\Delta a_i|}{a_i} \rightarrow \min \tag{A28}$$

The quantity ε is a measure of the numerical grid mismatch to the given geometric parameters and the pressure wave speed in individual pipes.

Confirmation that the applied method of discretization of the solution domain does not generate artificial numerical damping is shown in Figure A2 (immediate valve closure, flow

system configuration according to information contained in the table placed in Figure A2). The results of the pressure wave calculations obtained for the frictionless case show a constant amplitude of changes.

Calculations for different numerical grid densities for the configuration of the flow system as in the frictionless case presented in Figure A2 also confirmed that this parameter does not affect the obtained results. The following grid densities were used in the tests:

- grid size $72 \times 12,000$ ($0.864 \cdot 10^6$ nodes: $\Delta t = 0.00125$ s, $\Delta x_1 = 1.25$ m, $\Delta x_2 = 1.5$ m)
- grid size $180 \times 30,000$ ($5.4 \cdot 10^6$ nodes: $\Delta t = 0.0005$ s, $\Delta x_1 = 0.5$ m, $\Delta x_2 = 0.6$ m)
- grid size $450 \times 75,000$ ($33.75 \cdot 10^6$ nodes: $\Delta t = 0.0002$ s, $\Delta x_1 = 0.2$ m, $\Delta x_2 = 0.24$ m)

The obtained results did not show any visible differences in the generated numerical waveforms of the water hammer.

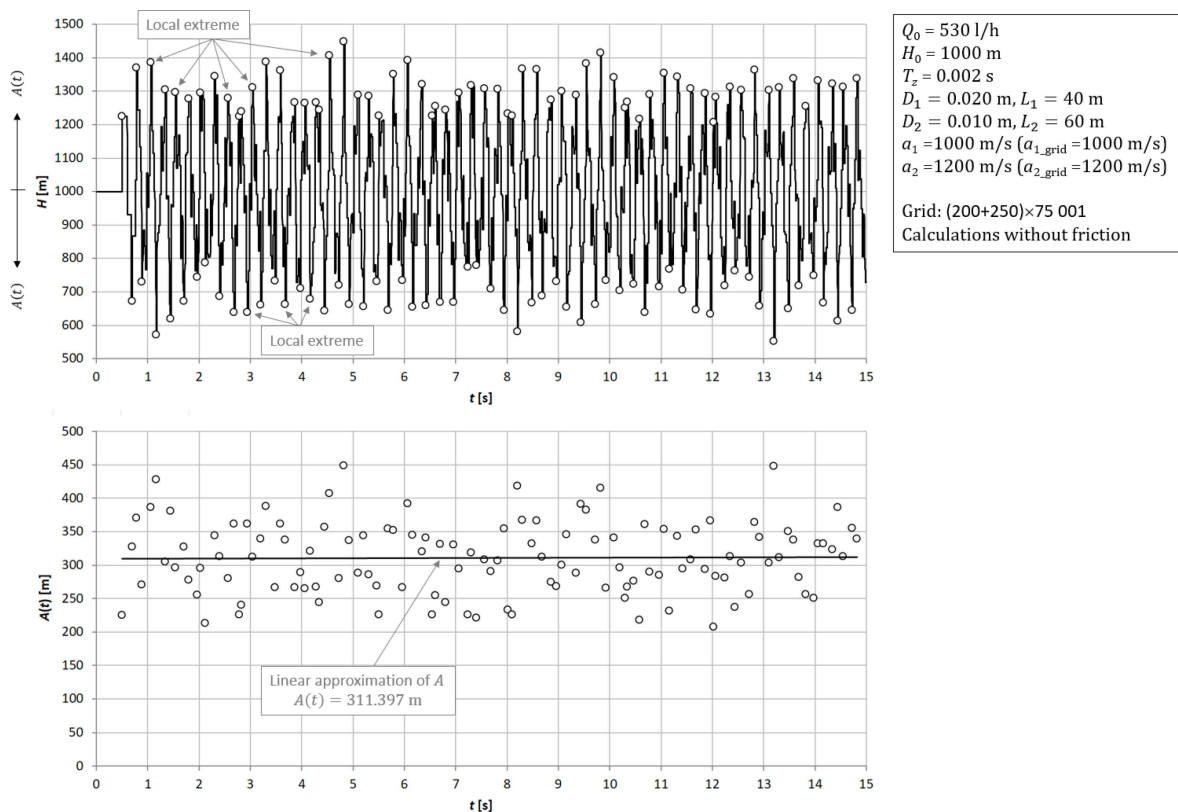


Figure A2. Pressure changes at the valve during water hammer in two series-connected pipes of different diameters. Calculations for frictionless case, using the own method of discretization of the solution domain. **Top** graph—pressure changes over time; **Bottom** graph—changes in pressure amplitudes over time and their linear approximation.

References

1. Meniconi, S.; Duan, H.F.; Brunone, B.; Ghidaoui, M.S.; Lee, P.J.; Ferrante, M. Further developments in rapidly decelerating turbulent pipe flow modeling. *J. Hydraul. Eng.* **2014**, *140*, 4014028. [[CrossRef](#)]
2. Mitosek, M.; Szymkiewicz, R. Wave Damping and Smoothing in the Unsteady Pipe Flow. *J. Hydraul. Eng.* **2012**, *138*, 619–628. [[CrossRef](#)]
3. Adamkowski, A.; Lewandowski, M. Experimental examination of unsteady friction models for transient pipe flow simulation. *ASME J. Fluid Eng.* **2006**, *128*, 1351–1363. [[CrossRef](#)]
4. Duan, H.F.; Ghidaoui, M.S.; Lee, P.J.; Tung, Y.K. Relevance of unsteady friction to pipe size and length in pipe fluid transients. *J. Hydraul. Eng.* **2012**, *138*, 154–166. [[CrossRef](#)]
5. Adamkowski, A.; Lewandowski, M. A new method for numerical prediction of liquid column separation accompanying hydraulic transients in pipelines. *ASME J. Fluid Eng.* **2009**, *131*, 071302-1–071302-11. [[CrossRef](#)]
6. Adamkowski, A.; Lewandowski, M. Investigation of Hydraulic Transients in a Pipeline with Column Separation. *ASCE J. Hydraul. Eng.* **2012**, *138*, 935–944. [[CrossRef](#)]

7. Adamkowski, A.; Lewandowski, M.; Marcinkiewicz, J. New method for numerical prediction of waterhammer with column separation—Comparison with experiment and the Relap5 program. In Proceedings of the 17th International Conference on Nuclear Engineering, Brussels, Belgium, 12–16 July 2009; pp. 1–8.
8. Karadžić, U.; Bulatovic, V.; Bergant, A. Valve-induced waterhammer and column separation in a pipeline apparatus. *Stroj. Vestn.-J. Mech. Eng.* **2014**, *60*, 742–754. [[CrossRef](#)]
9. Chen, Q.; Wang, L. Production of large size single transient cavitation bubbles with tube arrest method. *Chin. Phys.* **2014**, *13*, 564.
10. Oliveira, G.M.; Franco, A.T.; Negrão, C.O.R. Mathematical Model for Viscoplastic Fluid Hammer. *J. Fluids Eng. Trans. ASME* **2016**, *138*, 011301. [[CrossRef](#)]
11. Pezzinga, G.; Brunone, B.; Cannizzaro, D.; Ferrante, M.; Meniconi, S.; Berni, A. Two-dimensional features of viscoelastic models of pipe transients. *J. Hydraul. Eng.* **2014**, *140*, 04014036. [[CrossRef](#)]
12. Henclik, S. Numerical modeling of waterhammer with fluid–structure interaction in a pipeline with viscoelastic supports. *J. Fluids Struct.* **2018**, *76*, 469–487. [[CrossRef](#)]
13. Adamkowski, A.; Henclik, S.; Janicki, W.; Lewandowski, M. The influence of pipeline support stiffness onto the waterhammer run. *Eur. J. Mech. B/Fluids* **2017**, *61*, 297–303. [[CrossRef](#)]
14. Keramat, A.; Tijsseling, A.S.; Hou, Q.; Ahmadi, A. Fluid–structure interaction with pipe-wall viscoelasticity during waterhammer. *J. Fluids Struct.* **2012**, *28*, 434–455. [[CrossRef](#)]
15. Ivljanin, B.; Stevanovic, V.D.; Gajic, A. Waterhammer with non-equilibrium gas release. *Int. J. Press. Vessel. Pip.* **2018**, *165*, 229–240. [[CrossRef](#)]
16. Hatcher, T.M.; Vasconcelos, J.G. Peak pressure surges and pressure damping following sudden air pocket compression. *J. Hydraul. Eng.* **2017**, *143*, 04016094. [[CrossRef](#)]
17. Bergant, A.; Tijsseling, A.; Kim, Y.; Karadžić, U.; Zhou, L.; Lambert, M.; Simpson, A. Unsteady pressure influenced by trapped air pocket in liquid-filled pipelines. *Stroj. Vestn.-J. Mech. Eng.* **2018**, *64*, 501–512.
18. Lee, N.H.; Martin, C.S. Experimental and analytical investigation of entrapped air in a horizontal pipe. In Proceedings of the 3rd ASME/JSM E Joint Fluids Engineering Conference, San Francisco, CA, USA, 18–23 July 1999; pp. 1–8.
19. Wylie, E.B.; Streeter, V.L.; Suo, L. *Fluid Transients in Systems*; Prentice Hall: Hoboken, NJ, USA, 1993.
20. Zaruba, J. *Waterhammer in Pipeline Systems*; Developments in Water Science; Elsevier: Amsterdam, The Netherlands, 1993; Volume 43.
21. Raczynski, A.; Kirkpatrick, W.; Rehnstrom, D.; Boulos, P.; Lansey, K. Developing hydraulic and water quality equivalent systems. In Proceedings of the 10th Annual Water Distribution Systems Analysis Conference, Kruger National Park, South Africa, 17–20 August 2008; WDSA2008.
22. Mohammed, H.I.; Gad, A.A.M. Effect of pipes networks simplification on waterhammer phenomenon. *J. Eng. Sci. Assiut Univ.* **2012**, *40*, 1625–1647.
23. Adamkowski, A. Analysis of transient flow in pipes with expending or contracting sections. *ASME J. Fluid Eng.* **2003**, *125*, 716–722. [[CrossRef](#)]
24. Wu, T.; Ferng, C.-C. Effect of nonuniform conduit section on waterhammer. *Acta Mech.* **1999**, *137*, 137–149. [[CrossRef](#)]
25. Meniconi, S.; Brunone, B.; Ferrante, M. Water-Hammer Pressure Waves Interaction at Cross-Section Changes in Series in Viscoelastic Pipes. *J. Fluids Struct.* **2012**, *33*, 44–58. [[CrossRef](#)]
26. Triki, A. Water-Hammer Control in Pressurized-Pipe Flow Using an in-Line Polymeric Short-Section. *Acta Mech.* **2016**, *227*, 777–793. [[CrossRef](#)]
27. Ferrante, M. Transients in a Series of Two Polymeric Pipes of Different Materials. *J. Hydraul. Res.* **2021**, *59*, 810–819. [[CrossRef](#)]
28. Kubrak, M.; Malesińska, A.; Kodura, A.; Urbanowicz, K.; Stosiak, M. Hydraulic Transients in Viscoelastic Pipeline System with Sudden Cross-Section Changes. *Energies* **2021**, *14*, 4071. [[CrossRef](#)]
29. Kubrak, M.; Kodura, A.; Malesińska, A.; Urbanowicz, K. Waterhammer in Steel–Plastic Pipes Connected in Series. *Water* **2022**, *14*, 3107. [[CrossRef](#)]
30. Wan, W.; Huang, W. Waterhammer simulation of a series pipe system using the MacCormack time marching scheme. *Acta Mech.* **2018**, *229*, 3143–3160. [[CrossRef](#)]
31. Malesińska, A.; Kubrak, M.; Rogulski, M.; Puntorieri, P.; Fiamma, V.; Barbaro, G. Waterhammer Simulation in a Steel Pipeline System with a Sudden Cross Section Change. *J. Fluids Eng.-Trans. ASME* **2021**, *143*, 091204. [[CrossRef](#)]
32. Malesińska, A.; Rogulski, M.W.; Puntorieri, P.; Barbaro, G.; Kowalska, B.E. Equivalent Speed in Waterhammer for Series-Connected Pipelines. *J. Pipeline Syst. Eng. Pract.* **2020**, *11*, 04019039. [[CrossRef](#)]
33. Malesińska, A.; Rogulski, M.; Puntorieri, P.; Barbaro, G.; Kowalska, B.E. Use of Equivalent Speed to Estimate Maximum Pressure Increase in Serial Pipes during Waterhammer—Numerical Simulations in Matlab. *Int. J. Comp. Meth. Exp. Meas.* **2019**, *7*, 22–32.
34. Chaudhry, M.H. *Applied Hydraulic Transients*, 3rd ed.; Springer: New York, NY, USA, 2014. [[CrossRef](#)]
35. Duan, H.F.; Lee, P.J.; Ghidaoui, M.S.; Tung, Y.K. Extended Blockage Detection in Pipelines by Using the System Frequency Response Analysis. *J. Water Resour. Plan. Manag.* **2012**, *138*, 55–62. [[CrossRef](#)]
36. Duan, H.F.; Lee, P.J.; Kashima, A.; Lu, J.; Ghidaoui, M.S.; Tung, Y.K. Extended blockage detection in pipes using the system frequency response: Analytical analysis and experimental verification. *J. Hydraul. Eng.* **2013**, *139*, 763–771. [[CrossRef](#)]
37. Duan, H.F.; Lee, P.J.; Ghidaoui, M.S.; Tuck, J. Transient wave-blockage interaction and extended blockage detection in elastic water pipelines. *J. Fluids Struct.* **2014**, *46*, 2–16. [[CrossRef](#)]

38. Louati, M.; Meniconi, M.; Ghidaoui, M.S.; Brunone, B. Experimental study of the eigenfrequency shift mechanism in blocked pipe system. *J. Hydraul. Eng.* **2017**, *143*, 04017044. [[CrossRef](#)]
39. Louati, M.; Meniconi, S.; Ghidaoui, M.S.; Brunone, B. Bragg-Type Resonance in Blocked Pipe System and Its Effect on the Eigenfrequency Shift. *J. Hydraul. Eng.* **2018**, *141*, 04017056. [[CrossRef](#)]
40. Lee, P.J.; Duan, H.F.; Tuck, J.; Ghidaoui, M. Numerical and experimental study on the effect of signal bandwidth on pipe assessment using fluid transients. *J. Hydraul. Eng.* **2015**, *141*, 04014074. [[CrossRef](#)]
41. Tuck, J.; Lee, P.J.; Davidson, M.; Ghidaoui, M.S. Analysis of transient signals in simple pipeline systems with an extended blockage. *J. Hydraul. Res.* **2013**, *51*, 623–633. [[CrossRef](#)]
42. Brunone, B.; Ferrante, M.; Meniconi, S. Discussion of detection of partial blockage in single pipelines. *J. Hydraul. Eng.* **2008**, *134*, 872–874. [[CrossRef](#)]
43. Meniconi, S.; Brunone, B.; Ferrante, M.; Massari, C. Small amplitude sharp pressure waves to diagnose pipe systems. *Water Resour. Manag.* **2011**, *25*, 79–96. [[CrossRef](#)]
44. Massari, C.; Yeh, T.C.; Ferrante, M.; Brunone, B.; Meniconi, S. A stochastic approach for extended partial blockage detection in viscoelastic pipelines: Numerical and laboratory experiments. *J. Water Supply Res. Technol.* **2015**, *64*, 583–595. [[CrossRef](#)]
45. Meniconi, S.; Duan, H.F.; Lee, P.J.; Brunone, B.; Ghidaoui, M.S.; Ferrante, M. Experimental investigation of coupled frequency and time-domain transient test-based techniques for partial blockage detection in pipelines. *J. Hydraul. Eng.* **2013**, *139*, 1033–1040. [[CrossRef](#)]
46. Wylie, E.B.; Streeter, V.L. *Fluids Transients*; McGraw-Hill: New York, NY, USA, 1978.
47. *ISO/IEC GUIDE 98-3:2008; Uncertainty of Measurement—Part 3: Guide to the Expression of Uncertainty in Measurement (GUM:1995)*. ISO: Geneva, Switzerland, 2008.
48. Joukowsky, N. Über den hydraulischen Stoss in Wasserleitungsröhren [On hydraulic shock in water pipes]. In *Mémoires de l'Académie Impériale des Sciences de St.-Petersbourg*; 8th Series; Académie des sciences de Saint-Petersbourg: St. Petersburg, Russia, 1900; Volume 9, pp. 1–71. (In German)
49. Bahadori, A.; Vuthaluru, H.B. Prediction of bulk modulus and volumetric expansion coefficient of water for leak tightness test of pipelines. *Int. J. Press. Vessel. Pip.* **2009**, *86*, 550–554. [[CrossRef](#)]
50. Adamkowski, A.; Lewandowski, M. Cavitation Characteristics of Shutoff Valves in Numerical Modeling of Transients in Pipelines with Column Separation. *ASCE J. Hydraul. Eng.* **2014**, *141*, 04014077. [[CrossRef](#)]
51. Courant, R.; Friedrichs, K.; Lewy, H. Über die partiellen Differenzgleichungen der mathematischen Physik (On the partial difference equations of mathematical physics). *Math. Ann.* **1928**, *100*, 32–74. (In German) [[CrossRef](#)]
52. Vardy, A.E.; Brown, J.M.B. Transient turbulent friction in smooth pipe flows. *J. Sound Vib.* **2003**, *259*, 1011–1036. [[CrossRef](#)]
53. Vítkovský, J.; Stephens, M.; Bergant, A.; Lambert, M.; Simpson, A.R. Efficient and accurate calculation of Zielke and Vardy-Brown unsteady friction in pipe transients. In *Proceedings of the 9th International Conference on Pressure Surges*, Chester, UK, 24–26 March 2004; Murray, S.J., Ed.; BHR Group: Shahapur, Indian, 2004; Volume II, pp. 405–419.
54. Brunone, B.; Golia, U.M.; Greco, M. Modelling of Fast Transients by Numerical Methods. In *Proceedings of the International Meeting on Hydraulic Transients with Water Column Separation, 9th Round Table, IAHR, Valencia, Spain, 4–6 September 1991*; pp. 273–280.
55. Brunone, B.; Golia, U.M.; Greco, M. Some remarks on the momentum equation for fast transients. In *Proceedings of the International Meeting on Hydraulic Transients with Column Separation, 9th Round Table, IAHR, Valencia, Spain, 4–6 September 1991*; pp. 140–148.
56. Thomson, W.T. *Theory of Vibration with Applications*, 4th ed.; CRC Press: Boca Raton, FL, USA, 1993. [[CrossRef](#)]
57. Meirovitch, L. *Fundamentals of Vibrations*; McGraw-Hill: New York, NY, USA, 2001; p. 806.
58. Suter, S.P.; Skalak, R. The History of Poiseuille's Law. *Annu. Rev. Fluid Mech.* **1993**, *25*, 1–19. [[CrossRef](#)]

Disclaimer/Publisher's Note: The statements, opinions and data contained in all publications are solely those of the individual author(s) and contributor(s) and not of MDPI and/or the editor(s). MDPI and/or the editor(s) disclaim responsibility for any injury to people or property resulting from any ideas, methods, instructions or products referred to in the content.